Deglaciation of a major palaeo-ice stream in Disko Trough, West Greenland

Kelly A. Hogan [a, *], Colm Ó Cofaigh [b], Anne E. Jennings [c], Julian A. Dowdeswell [d], John F. Hiemstra [e]

[a] British Antarctic Survey, Natural Environmental Research Council, High Cross, Madingley Road, Cambridge, CB3 0ET, UK
[b] Department of Geography, Durham University, Science Laboratories, South Road, Durham DH1 3LE, UK
[c] INSTAAR and Department of Geological Sciences, University of Colorado, Boulder, CO 80309-0450, USA
[d] Scott Polar Research Institute, University of Cambridge, Lensfield Road, Cambridge, CB2 1ER, UK
[e] Department of Geography, College of Science, Swansea University, Singleton Park, Swansea, SA2 8PP, UK

ARTICLE INFO

ABSTRACT

Recent work has confirmed that grounded ice reached the shelf break in central West Greenland during the Last Glacial Maximum (LGM). Here we use a combination of marine sediment-core data, including glacimarine lithofacies and IRD proxy records, and geomorphological and acoustic facies evidence to examine the nature of and controls on the retreat of a major outlet of the western sector of the Greenland Ice Sheet (GrIS) across the shelf. Retreat of this outlet, which contained the ancestral Jakobshavns Isbræ ice stream, from the outer shelf in Disko Trough was rapid and progressed predominantly through iceberg calving, however, minor pauses in retreat (tens of years) occurred on the middle shelf at a trough narrowing forming subtle grounding-zone wedges. By 12.1 cal kyr BP ice had retreated to a basalt escarpment and shallow banks on the inner continental shelf, where it was pinned and stabilised for at least 100 years. During this time the ice margin appears to have formed a calving bay over the trough and melting became an important mechanism of ice-mass loss. Fine-grained sediments (muds) were deposited alternately with IRD-rich sediments (diamictons) forming a characteristic deglacial lithofacies that may be related to seasonal climatic cycles. High influxes of subglacial meltwater, emanating from the nearby ice margins, deposited muddy sediments during the warmer summer months whereas winters were dominated by iceberg calving leading to the deposition of the diamictons. This is the first example of this glacimarine lithofacies from a continental-shelf setting and we suggest that the calving-bay configuration of the ice margin, plus the switching between calving and melting as ablation mechanisms, facilitated its deposition by channelling meltwater and icebergs through the inner trough. The occurrence of a major stillstand on the inner shelf in Disko Trough demonstrates that the ice-dynamical response to local topography was a crucial control on the behaviour of a major outlet in this sector of the GrIS during retreat.

1. Introduction

During the Last Glacial Maximum (LGM) in Greenland (24—16 ka BP; Funder et al., 2011) ice expanded onto the adjacent continental shelves, although how far the ice sheet extended across the shelf is still a matter of debate in many areas. Based on coastal landforms and, less often, evidence from marine geophysical datasets, ice-sheet reconstructions indicate that the LGM Greenland Ice Sheet (GrIS) was drained at its periphery by a number of confluent ice streams and outlet glaciers (e.g. Evans et al., 2002; 2009; Winkelmann et al., 2010; Roberts and Long, 2005; Roberts et al., 2009; 2010; 2013), at least some of which extended to the shelf break in the cross-shelf troughs that dissect the Greenland continental margin (e.g. Dowdeswell et al., 2010; 2014; Ó Cofaigh et al., 2013a). These fast-flowing corridors of ice must have been a critical factor affecting the mass balance of the ice sheet, in particular during deglaciation, because they would have dominated the overall discharge in the same way that ice streams and outlet glaciers do for ice sheets today (cf. Bamber et al., 2000; Bennett, 2003).

* Corresponding author.
  E-mail address: kelgan@bas.ac.uk (K.A. Hogan).

Reconstructing the retreat patterns and chronologies of major marine-terminating outlets since the LGM provides centennial-to-millennial-scale records of their behaviour in response to a variety of factors including climatic change and ice-dynamical controls. Improved understanding of these controls is critical in order to increase our ability to predict future responses of the polar ice sheets to ongoing climate change (cf. Velicogna, 2009; Nick et al., 2013). Such palaeo-records also serve as important long-term context for recent and ongoing ice-sheet change, which is occurring today through the thinning and retreat of marine-terminating outlet glaciers and ice streams, in Northwest and Southeast Greenland (Rignot and Kanagaratnam, 2006; Moon et al., 2008; Khan et al., 2010; Velicogna, 2009) and around West Antarctica (Joughin et al., 2003; Rignot et al., 2014).

Generating new records of ice retreat from offshore areas in central West Greenland in particular is important for several reasons. Firstly, a large amount of terrestrial geomorphological and deglacial chronological data is available for the Disko Bugt and Sisimiut regions (Weidick, 1972; Kelly, 1985; Funder, 1989); this is because this area is an important drainage route for the modern GrIS via the Jakobshavns Isbræ ice stream, which drains c. 7% of the ice sheet (Joughin et al., 2004). Despite this, information on how the ice sheet was configured on the wide continental shelf in the past, and how and when it deglaciated, is only just emerging (Ó Cofaigh et al., 2013a; Dowdeswell et al., 2014; Jennings et al., 2013; Rinterknecht et al., 2014; Sheldon et al., 2016). Furthermore, based on onshore and offshore deglacial chronologies around Greenland it is clear that the final retreat of the GrIS after the LGM was asynchronous, and that it was influenced by both topographic effects and local ice-sheet dynamics, and was not driven solely by climatic change (Bennike and Björck, 2002; Funder et al., 2011; Ó Cofaigh et al., 2013a). Identifying and understanding this asynchronicity provides important new information on the behaviour of the GrIS during periods of climatic warming, as well as insights into the dynamic response of ice sheets and their outlets on timescales longer than the observational record.

This paper integrates sediment-core data from 10 marine cores with multibeam-bathymetric data and high-resolution acoustic profiles acquired in Disko Trough during cruise JR175 to central West Greenland in 2009. By generating sedimentary lithofacies, IRD proxy, and acoustic facies datasets we determine the style and relative rates of retreat of a major GrIS outlet from its Younger Dryas maximum on the outer shelf, and we examine the importance of local topography on the stability of the outlet's grounded margin during deglaciation. This study also forms part of a wider research agenda to investigate the nature and behaviour of western GrIS ice streams and outlet glaciers over the last glacial-deglacial cycle (Hogan et al., 2011; 2012; Ó Cofaigh et al., 2013a; b; Dowdeswell et al., 2014) and the palaeoenvironmental conditions influencing ice-sheet decay (Lloyd et al., 2005; 2011; Perner et al., 2011; McCarthy, 2011; Jennings et al., 2013; Sheldon et al., 2016) from marine geophysical and geological datasets. The work fills an important gap in our knowledge of Greenland's glacial history from offshore areas surrounding the landmass (cf. Funder et al., 2011) and compliments the wealth of terrestrial studies available in the literature (see, for example, Weidick, 1972; Kelly, 1985; Funder, 1989; Bennike and Björck, 2002; Funder and Hansen, 1996, and references therein).

1.1. Regional setting

Disko Trough is a large bathymetric trough that crosses the continental shelf offshore central West Greenland at around 68° 24′N (Fig. 1). The broad, generally u-shaped cross-profile of the trough (Fig. 1b) is evidence that it has been eroded by glacial ice;

however, the trough appears to be fault-bounded on its northern side (Hofman et al., 2016) and most authors believe that successive Quaternary ice advances have followed an older (Pre-Quaternary) drainage system on the shelf (Henderson, 1975; Funder and Larsen, 1989). The trough extends for 195 km from a basalt escarpment on the inner shelf to the outer shelf where there is a small dog-leg diverting the trough axis to the south-west (Fig. 1). Trough width is typically around 40 km but it is variable along its length, with a notable narrowing on the mid-shelf (57° 15′W), east of which the trough widens and deepens; water depths are generally between 400 and 550 m on the mid-outer shelf. On the inner shelf, the trough is flanked by relatively shallow banks: Disko Banke to the north has typical water depths of 150–250 m, and Store-Hellefiske Banke to the south has water depths of <50 m—200 m. The shallow banks and escarpment on the inner shelf comprise Palaeogene basalts (Chalmers et al., 1999; Larsen and Pulvertaft, 2000), whereas the continental shelf consists of prograded beds of Late Cretaceous-Quaternary sediments (Rolle, 1985; Hofman et al., 2016). East of the basalt escarpment, over which water depths shallow to 300–350 m, is a NNE-SSW trending trough - Egedesminde Dyb - that connects Disko Trough to the Disko Bugt embayment. Taken together, this trough-bay system has a sinuous or "kinked" central axis suggesting that former ice flow of any expanded ice sheet draining through this system may have been strongly affected by topography (cf. Long and Roberts, 2003). At present, water masses on the central West Greenland shelf are dominated by the relatively warm, saline West Greenland Current (WGC), an admixture of the North Atlantic Irminger Current and the East Greenland Current (EGC) (Buch, 1981). The WGC flows northwards over the entire West Greenland shelf, although cold, low-salinity water originating in the EGC, dominates surface waters near the coast (Ribergaard and Buch, 2008).

The traditional view of LGM glaciation in central West Greenland, locally termed the Sisimiut Stade (Kelly, 1985), places the ice-sheet margin at the Fiskebanke moraines which lie on the inner shelf between 10 and 50 km from the coast south of 68°N (Brett and Zarudzki, 1979; Roksandic, 1979). A further set of moraines, the Hellefiske moraines, is found on the outer shelf in southwest Greenland but lies on the middle shelf in central West Greenland (Fig. 1) (Funder and Larsen, 1989). The Hellefiske moraines are usually assigned a Saalian age and the Fiskebanke moraines a Sisimuit age based on correlation of the latter moraines with coastal weathering limits (Kelly, 1985), and extrapolation across the shelf from coastal ice thicknesses (see Funder, 1989; Funder and Hansen, 1996; Funder et al., 2011). However, several studies have since suggested that the LGM margin may instead have extended to the shelf break (e.g. van Tatenhove et al., 1996; Weidick et al., 2004; Roberts et al., 2009), and the compromise view is of a LGM GrIS extending to a limit at the inner shelf moraines with the possibility of ice extending to the shelf break particularly in glacial troughs where increased ice thicknesses and discharge may have promoted ice-stream stability (Long and Roberts, 2002; Roberts et al., 2009). Recent studies from the continental shelf confirm that the GrIS did indeed expand on to the outer shelf in both the Disko and Uummannaq cross-shelf trough systems (Ó Cofaigh et al., 2013a; Dowdeswell et al., 2014). On land, glacially-sculpted landforms suggest that ice in the troughs was fed by confluent ice streams draining into one main outlet on the inner shelf (Roberts and Long, 2005; Roberts et al., 2013); this preferential drawdown of ice into the troughs has been cited as a possible explanation for the widespread evidence of only thin ice at the coastline (Roberts et al., 2013). Ice occupying Disko Trough during the LGM is thought to have been fed by several outlets including the ancestral Jakobshavns Isbræ (ice stream) indicating that the trough was an important drainage route for the GrIS (e.g. Ó Cofaigh et al.,
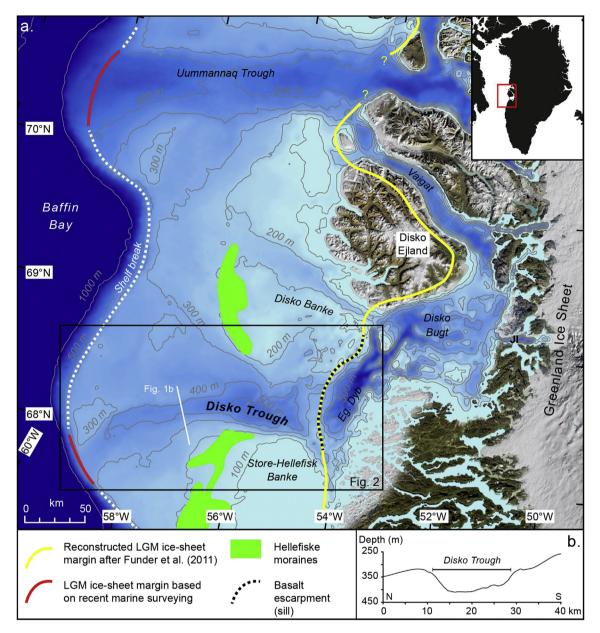
Fig. 1. (a) Overview map of Disko Trough and the offshore areas of central West Greenland including major moraines on the shelf and the location of the basalt escarpment at the eastern end of Disko Trough. Also shown is the reconstructed LGM ice margins after Funder et al. (2011) and reconstructed ice-stream margins in Disko and Uummannaq Troughs following recent marine surveying (Ó Cofaigh et al., 2013a; Jennings et al., 2013; Dowdeswell et al., 2014). The imagery over land areas is a 250-m resolution MODIS mosaic produced by Paul Morin using MODIS data from the LANCE (Rapidfire) project (http://rapidfire.sci.gsfc.nasa.gov/subsets/?mosaic=Arctic). Some residual snowy areas remain on the south side of Disko Bay and the west side of Disko Ejland. Regional bathymetry is from IBCAO v. 3.0 (Jakobsson et al., 2012). JI: Jakobshavns Isfjord; Eg. Dyb.: Egedesminde Dyb. (b) Seafloor profile over Disko Trough on the mid-shelf, location in (a).

2013a; Roberts and Long, 2005; Weidick and Bennike, 2007).

Radiocarbon dates from marine-sediment cores provide constraining dates for the withdrawal of ice. Ó Cofaigh et al. (2013a) showed that retreat from the shelf break in Disko Trough was well underway by 13.8 cal kyr BP, but that a short-lived readvance on the outer shelf occurred during the Younger Dryas (YD) and was followed by rapid retreat after 12.2 cal kyr BP. Using a range of palaeoenvironmental proxy data, Jennings et al. (2013) documented cold oceanographic conditions during retreat from the outer shelf with near permanent sea-ice cover, and no evidence of warm ocean currents entering Disko Trough that may have promoted or enhanced ice decay. Ice-mass loss was predominantly through calving during this rapid retreat phase (Ó Cofaigh et al.,

2013a; Jennings et al., 2013). East of the basalt escarpment on the inner shelf, grounded ice had withdrawn from Egedesminde Dyb by 11.1 kyr BP (Kelley et al., 2013), and from eastern Disko Bugt by 10.3 cal kyr BP (Lloyd et al., 2005) indicating that retreat from the inner shelf to the present-day coastline was much slower than retreat across the continental shelf. At the mouth of Jakobshavns Isfjord the ice margin readvanced or paused around 9.2 kyr BP forming the Marriat moraine system (Young et al., 2011; 2013); offshore the ice margin likely stabilised at a semi-circular submarine bank at the fjord-mouth at this time (Hogan et al., 2012).

2. Materials and methods

The data used to reconstruct the style of, and factors influencing deglaciation in Disko Trough consist of 10 marine sediment cores (vibrocores; Table 1), gridded multibeam-bathymetric soundings providing a 3D digital terrain model of the seafloor, and high-resolution acoustic profiles imaging the sub-seafloor sediment units (Fig. 2). These datasets were collected during a NERC-funded research cruise (JR175) of the RSS *James Clark Ross* in August−September 2009. New chronological information for VC24, VC21, and VC01 is based on calibrated radiocarbon dates; previously published dates from Ó Cofaigh et al. (2013a), Jennings et al. (2013) and McCarthy (2011) were also recalibrated in order to be directly comparable to the new dates presented here (see details below).

2.1. Geophysical data

The multibeam-bathymetric data was acquired with a Kongsberg EM120 echosounder operating with a frequency of 12 kHz and emitting 191 across-track beams per ping. The echosounder was run in a 1° by 1° configuration in water depths of between 200 and 600 m in Disko Trough leading to a spatial density of soundings from the seafloor that allowed data to be gridded with cell-sizes of 30−40 m. Bathymetric soundings were processed using a combination of MB-System and Fledermaus software to correct edge artefacts due to the use of poor sound-velocity profiles and to remove spurious data points. High-resolution seismic profiles were acquired concomitantly with the multibeam dataset along the centreline of the swath. These data were collected using a Kongsberg parametric sub-bottom profiler (TOPAS) which has primary frequencies of 15−21 kHz (centred at 18 kHz) and produces a secondary waveform with frequencies between 0.5 and 6 kHz. In the soft seafloor sediments that occur in parts of Disko Trough penetration was up to 50 m below the seafloor; vertical resolution of the data is on the order of a few tens of cm.

2.2. Vibrocores

All vibrocores were acquired using the British geological Survey's corer with a 6-m barrel; core recovery was good with full recovery in soft sediments and penetration of subglacial till in some cores. Lithofacies descriptions and interpretations are based on visual core logs and inspection of x-radiographs of split cores for sedimentary structures including grading, contacts, outsized clast content, deformation structures, bioturbation and the occurrence of mollusc shells. Here we are primarily interested in the deglacial or "transitional" glacimarine units, typically consisting of gravelly-sands or muds with coarse grains or granules, that are often deposited overlying subglacial (diamicton) till facies and stratigraphically below post-glacial (or distal glacimarine) hemipelagic mud facies (cf. Vorren et al., 1984; Domack et al., 2005; Evans et al., 2005). The term diamicton in this paper refers to a poorly sorted admixture of muds, sands and clasts and does not carry an implication for the genesis of this facies, whereas the term till implies a glacial origin to the sediment (cf. Eyles et al., 1983). In the generally fine-grained units above subglacial tills, variations in ice-rafted debris (IRD) (i.e. clasts >2 mm diameter) are quantified as the number of clasts counted within 2-cm thick by 7-cm wide windows of the x-radiographs (Grobe, 1987). We note that because the x-radiographs are of split cores (rather than 2-cm slabs of sediment) the counts may be somewhat lower than reality as some clasts may be "hidden" behind the thickest sediment in the centre of the core or behind other clasts. Shear strength measurements made every 10 cm using a hand-held torvane are presented for cores VC19-21 and VC23-26. Magnetic susceptibility (MS) data are presented for VC20 and VC24 only, representing a core from the outer and inner parts of Disko Trough, respectively. These physical parameters were measured soon after core splitting at 1-cm intervals on a Geotek Multi-Sensor Core Logger at Durham University. Down-core variations in MS are interpreted to represent changes in the provenance of terrestrial sediments between those with higher contents of magnetic minerals and those with low magnetic mineral contents. In glacimarine settings, MS can also vary with changes in grain size (cf. Kilfeather et al., 2011) whereby larger magnetic particles return higher MS values. On the outer shelf likely sediment sources include Tertiary basalts from the inner shelf (high magnetic mineral contents) and Palaeozoic sedimentary sequences (low magnetic mineral contents) (Jennings et al., 2013; Andrews and Eberl, 2011). One thin section was produced of the basal unit of VC17, allowing the micromorphology of this unit to be analysed.

Data for core VC20 including sedimentary lithofacies, IRD counts, shear strength measurements, and radiocarbon dates have been presented by Ó Cofaigh et al. (2013a) and Jennings et al. (2013). Here we include only a brief summary of these previously-published data where applicable but we present new MS data for this core and consider the deglacial lithofacies in this core alongside the new results from the other 9 cores.

2.3. Chronology

For new radiocarbon dates from VC24, VC21, and VC01 we apply a ΔR of 140 ± 30 years for Disko Bugt following Lloyd et al. (2011) and Jennings et al. (2013). The dates were calibrated using the online program Calib 7.1 (Stuiver et al., 2015) with the Marine 13.14c calibration curve (Reimer et al., 2013). Although recalibration of the previously-published dates was performed using this most recent software and calibration curve to make sure that the dates were directly comparable, this did not alter the dates when rounded to the nearest 10 years and so the details of the recalibrated dates are not reported here. It is also acknowledged that the local reservoir effect, which is based on information from Disko Bugt - a coastal embayment - may not be appropriate for the middle-outer continental shelf and may have varied during deglaciation around Greenland (cf. Bennike and Björck, 2002). However, this is the best reservoir effect information that we have available at present. Average sedimentation rates were calculated for the lower parts of core VC21 and VC24 using the new dates and existing core chronologies.

Table 1
Site information for sediment cores from Disko Trough, West Greenland; core locations are shown in Fig. 1. *VC20 has been reported previously by Ó Cofaigh et al. (2013a) and Jennings et al. (2013) and these datasets are cited in the text and figures (see Methods for full description of new and previously published data for this core).

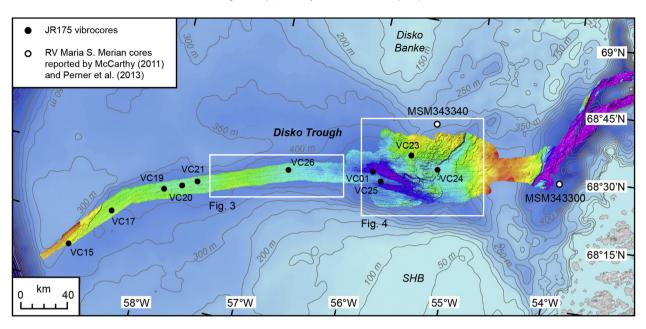| Core name	Latitude	Longitude	Water depth (m)	Length (cm)
VC01	68° 23.9′ N	55° 53.9′ W	545	270
VC15	67° 54.5′ N	58° 43.9′ W	347	55
VC17	68° 03.0′ N	58° 23.7′ W	399	82
VC19	68° 10.5′ N	57° 55.7′ W	415	204
VC20*	68° 12.1′ N	57° 45.4′ W	424	539
VC21	68° 13.7′ N	57° 37.0′ W	430	510
VC23	68° 29.0′ N	55° 32.6′ W	400	596
VC24	68° 26.9′ N	55° 15.2′ W	432	563
VC25	68° 22.0′ N	55° 47.8′ W	521	493
VC26	68° 20.5′ N	56° 44.6′ W	446	465

Fig. 2. Location of geological (vibrocore) and geophysical (multibeam-bathymetric) datasets in Disko Trough, and previously-reported core locations discussed in the text. SHB: Store-Hellefiske Banke. The locations of subsequent figures are also shown.

3. Results and interpretation

3.1. Submarine landforms

3.1.1. Subtle transverse sediment ridges

Description: On the middle shelf in Disko Trough, between about 57°30′ W and 56° 25′ W, are several subtle ridges or scarps oriented transverse to the trough axis or slightly oblique to it (Fig. 3). Acoustic profiles show faint sub-bottom reflections beneath the ridges indicating that they comprise wedges of unconsolidated sediments (Fig. 3b). The western ridge (GZW1) is broad and has a subdued and somewhat curved surface profile in cross-section (Fig. 3b); the ridge has a shorter west-facing flank and a longer east-facing flank implying asymmetry. However, both flanks have low average slope gradients around 0.1° with the western slope being slightly steeper (after adjustment by removing the regional seafloor slope). The height of the ridge is around 25 m. Around 56°25′ W are two subtle ridges (here termed the central and eastern ridges; GZWs 2 and 3 on Fig. 3) around 10 m in height and oriented NNW-SSE. The central ridge is asymmetrical with a steeper west-facing slope (average slope 0.9°) and a gentler east-facing slope (average 0.3°) whereas the eastern ridge is symmetrical in cross-section. The large western ridge is located at the crest of a landward-deepening section of Disko Trough and the two smaller ridges are situated on this slope (Fig. 3). The two smaller ridges are located around 35 km east of the large ridge and the small ridges are 6 km apart (crest to crest spacing).

On sub-bottom profiles the top of the ridges and sedimentary wedges that underlie them are defined by a relatively strong, prolonged reflection with an undulating surface; the wedges comprise acoustically-homogenous to acoustically-transparent material (Fig. 3b). Weak, discontinuous sub-bottom reflections are occasionally visible at depths of several tens of metres below the surface reflection. There are no other units overlying the western wedge (GZW 1) at its shallowest point, but on its east-facing slope is a conformable, homogenous to stratified unit, 5–20 m thick that thickens towards the east, i.e. in the overdeepened part of the trough.

Interpretation: The geometry of the western and central ridges,

which are oriented transverse to the axis of the glacial trough, are asymmetric in cross profile with steeper seaward-facing slopes, and are tens of metres thick, have characteristics similar to those of grounding-zone wedges (GZWs) (cf. Ottesen et al., 2005; 2007; Dowdeswell and Fugelli, 2012). GZWs form subglacially at the margins of grounded ice sheets during stillstands in their retreat, which allows for subglacial sediment to build up into a wedge-shaped sediment body along the grounding line (Alley et al., 1986). The ridges in Disko Trough are somewhat different from classic examples of GZWs from the Norwegian-Svalbard (e.g. Ottesen et al., 2005; 2007) and Antarctic continental margins (e.g. Larter and Vanneste, 1995; Anderson, 1999; Ó Cofaigh et al., 2005; Jakobsson et al., 2012) in that they have more subtle morphologies defining only broad ridges rather than distinct seaward-facing scarps (Fig. 6). Moreover, the ridges occur on a landward-dipping slope, which is somewhat unusual for GZWs on northern hemisphere glaciated margins. GZWs most often form at locations where palaeo-ice streams stabilised during retreat, for example, at topographic pinning points including trough constrictions and (or) shallowings (cf. Jamieson et al., 2014).

The morphology of the western ridge (GZW1 on Fig. 3), which is very wide in the direction of ice-flow (~35 km) and has low relief (<25 m), does not favour formation as a terminal moraine but it could be an older moraine ridge or GZW that has subsequently been overridden (e.g. Ottesen and Dowdeswell, 2006), although the ridge is wide compared to previously-described overridden moraines. The dimensions and asymmetry of the ridge are more consistent with an interpretation as a GZW. We may explain the subtle and rounded surface expression and the extreme width of this feature as a result of its position on the cusp of a reverse-bed slope. The cusp of the slope would further reduce the already limited accommodation space available for sediment deposition at the grounding zone, assuming that the grounding zone was indeed bounded by an ice shelf and that the wedge of material accumulated in a low-gradient, water-filled cavity beneath the ice shelf (Dowdeswell and Fugelli, 2012). Thus, a relatively thin wedge of subglacial material accumulated over a broad grounding zone, rather than building a pronounced positive relief feature.

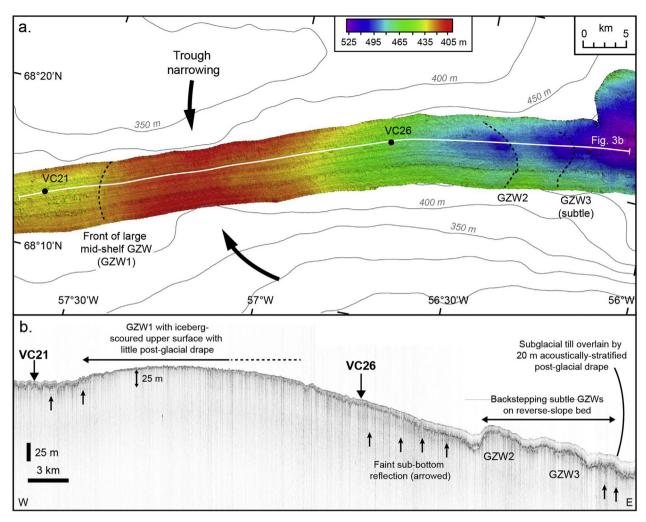Our preferred interpretation of the central and eastern ridges in

Fig. 3. (a) Multibeam-bathymetric shaded relief image of subtle sediment wedges interpreted as GZWs on the middle-continental shelf in Disko Trough. The front scarps of the GZWs are delineated with dashed lines and relevant vibrocore locations are shown. (b) TOPAS sub-bottom profile over the GZWs. A faint sub-bottom reflection (arrowed) indicates that the wedges consist of unlithified sedimentary material; for location see (a).

Disko Trough (GZWs 2 and 3 on Fig. 3) is as small GZWs deposited during stillstands in the retreat of an ice stream in Disko Trough, although their position on a reverse-bed slope is unusual. Minor GZWs with similar dimensions have recently been identified on the mid-shelf in Uummannaq Trough some 250 km to the north (Dowdeswell et al., 2014). The stratified to homogenous sediment unit overlying the wedges is a deglacial to post-glacial sediment drape deposited from suspension after grounded ice had retreated towards the east. These units correspond to the stratified muds and diamictons and homogeneous muds found in cores VC26 and VC01. Radiocarbon dates from the deglacial sediment units, although not from the area overlying the wedges, are all Holocene in age (Table 2, Jennings et al., 2013) implying that the wedges most likely formed following retreat of ice through the trough from the Younger Dryas extent on the outermost shelf (Ó Cofaigh et al., 2013a).

Given that ice-stream retreat was towards the east in Disko Trough, this means that the GZWs identified here occur on a reverse-bed slope. On reverse-bed slopes, in the absence of lateral drag, there is a strong positive feedback that promotes grounding-zone retreat by increasing strain rates and ice losses and destabi-lizing the grounding-line (Weertman, 1974; Schoof, 2007). How-ever, the regional bathymetry shows that Disko Trough does indeed narrow at the location of GZW1, and, thus lateral drag with the sides of the trough increased in this area and may have temporarily

stabilised the ice margin during retreat. GZW1 is also in line (outside of the trough) with the westward extension of the Store-Hellefiske Banke marked by the 200 m contour to the south of the trough, and with a shallow bank (300–350 m deep) on the north side of the trough (Figs. 2 and 3). Constriction of the trough width and these bathymetric features likely facilitated any short stillstand(s) during retreat on the mid-shelf.

3.1.2. Glacial lineations

3.1.2.1. Description. On the inner shelf there is a small area around 55° 45′W of lineated terrain comprising linear ridges 5–10 m high, several hundred metres wide and extending for between 5 and 14 km (limited by the edge of the multibeam data) (Fig. 4a). One broader ridge (about 3 km wide) occurs in the deepest part of the trough but disappears to the west. At the eastern end of some of the ridges are streamlined peaks rising around 50 m from the sur-rounding seafloor. The streamlined peaks and ridges are oriented in an ENE-WSW direction. On TOPAS seismic profiles the upper sur-faces of the linear ridges and streamlined peaks are defined by a strong, continuous reflection that is more prolonged on the ridges; rare sub-bottom reflections can be identified beneath the edges of the linear ridges (Fig. 4c). The ridges and peaks are mantled by 5–10 m of acoustically-stratified to homogenous material.

Table 2
Radiocarbon dates for Disko Trough sediment cores. All dates were calibrated using a ΔR of 140 ± 30 following Lloyd et al. (2011), Jennings et al. (2013) and Ó Cofaigh et al. (2013a) and the calibration program Calib 7.1 with the Marine 13.14c dataset (Reimer et al., 2013). Median probability age is rounded to the nearest 10 years.

Core name	Depth in core (cm)	Carbon source (setting)	Lab. code	^{14}C age (B.P.)	1σ min. cal. age − max. Cal. age	2σ min. cal. age − max. Cal. age	Median calibrated age (cal. yr B.P.)
VC01	24.5	Small shell fragments	CURL-16085	1230 ± 20	624–681	565–716	653
VC01	180–181	Large shell fragments	CURL-16084	2785 ± 20	2290–2394	2207–2415	2332
VC21	460	Paired bivalve shell (*Macoma calcarea*)	Beta265216	10140 ± 50	10843–11122	10700–11195	10970
VC24	149–150	Single valve, pelecypod	CURL-16082	10525 ± 42	11290–11580	11235–11736	11460
VC24	165	(*Yoldiella intermedia*)	CURL-16666	10455 ± 42	11208–11393	11174–11615	11320
VC24	217–218	Paired bivalve shell (sp. not known)	CURL-17355	10680 ± 46	11657–11954	11423–12017	11780

3.1.2.2. Interpretation. The linear ridges with rounded protuberances at their eastern ends are interpreted as glacial lineations and crag-and-tails (e.g. Hogan et al., 2010; Rydningen et al., 2013) formed subglacially by ice flowing through Disko Trough. The drumlinised protuberances form the "crags" of the crag-and-tail features and confirm that ice flow was from east to west in the trough. The sub-bottom reflections seen on TOPAS profiles beneath the ridges suggest that the "tails" are composed of sediment, whereas the crags probably consist of bedrock (Fig. 4c).

3.1.3. Rugged seafloor and channels

3.1.3.1. Description. Between 56° W and 54°30′ W the bathymetry in Disko Trough varies sharply between 270 m water depth and 570 m depth (Fig. 4a). The shallow areas are characterised by a rugged morphology that has a N–S to NNE-SSW fabric defined by scalloped to sinuous scarps that are steep on their east-facing sides (3–14°) and dip gently (1–2°) on their western sides. The terrain is smoother in the east and west where rounded crags occur on shallow plateau or mounds and the linear fabric is less defined (Figs. 2 and 4a). On the eastern sides of several of the scarps and protuberances are well-defined curvilinear channels that bend around the seafloor highs. Cross-sections of the channels reveal that they are usually u-shaped in profile and can have flat bottoms; maximum widths and depths are around 600 m and 45 m, respectively. In other places the areas between the highs are overdeepened by several tens of metres to form either linear flat-bottomed depressions or linked cavity-depression systems. A second area of rugged seafloor, with scalloped or sinuous scarps up to 20 m high, is present on the outermost shelf (around 58°45′ W) in the bathymetry data (Fig. 2); here the escarpments trend NE-SW.

Sub-bottom profiles over the rugged seafloor and channels on the inner shelf show that this morphology is defined by a strong, continuous reflection that becomes more diffuse on steep slopes (Fig. 4b); no reflections are visible beneath this impenetrable reflection. The upper reflection is overlain by a 5–20 m thick acoustically-stratified, conformable unit (Fig. 4b, c).

3.1.3.2. Interpretation. The sinuous scarps with lineated terrain is easily interpreted as the eroded surface of Palaeogene flood basalts that are known to crop out at the seafloor on the inner shelf in central West Greenland (Chalmers et al., 1999; Bonow, 2005). The escarpments are probably the edges of individual sheet flows, which dip westwards with less than 5° angles in the Disko area (Brett and Zarudzki, 1979; Chalmers et al., 1999) that have presumably been plucked and drumlinised on their eastern sides by glacial ice that flowed over the area from east to west. Faulting may have also contributed to the formation of this rugged terrain (cf.

Rydningen et al., 2013). This exposed bedrock is mantled by the conformable sediment unit deposited from suspension after grounded ice had withdrawn from the area. The rugged seafloor on the outer shelf is probably where the multibeam coverage extends over the northern flank of Disko Trough, which has a dog-leg that turns towards the SW on the outer shelf (see Figs. 1 and 2). Here the scarps may represent erosion of Quaternary sediments exposed at the seafloor of central West Greenland (Whittaker et al., 1996; Hofman and Knutz, 2015). Based on seismic-reflection profiles Hofman and Knutz (2015) identified two buried palaeo-troughs on the Disko trough-mouth fan (TMF) and hypothesized that these depressions held glacier ice from an earlier glaciation. The recovery of sediments dated to just after the LGM on the southern part of Disko TMF (Ó Cofaigh et al., 2013a; b; Jennings et al., 2013) confirms grounded ice flow through the bathymetric dog-leg to the shelf break during the last glacial.
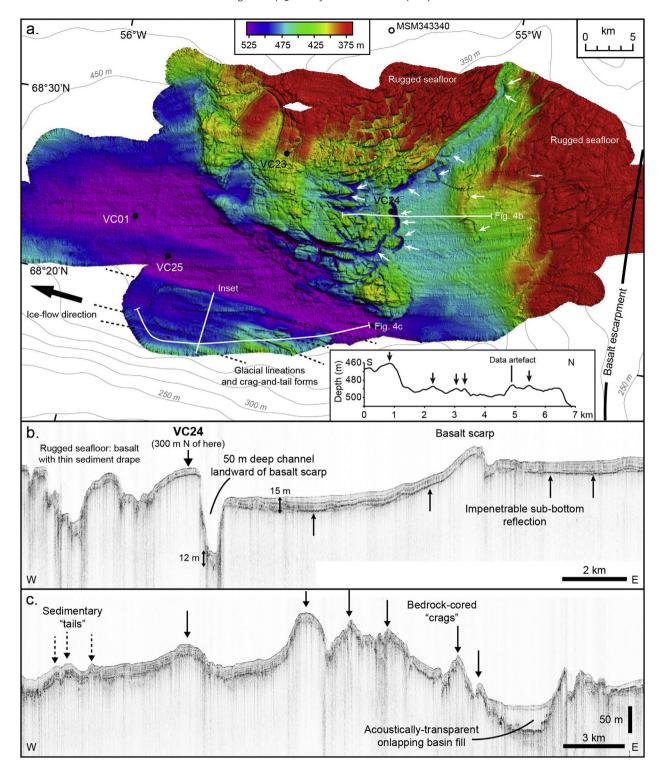
Overdeepenings in the channels, linear depressions and linked cavity-depression systems in the context of this glaciated landscape are indicative of subglacial erosion by meltwater, or a meltwater-sediment mixture. The pressure of the overlying ice allows fluid to flow along gradients in hydraulic potential that are independent of the underlying topography (Shreve, 1972) resulting in the formation of overdeepened sections. Thus, the channels and depressions in inner Disko Trough are interpreted as having been eroded by subglacial meltwater and sediment. The timing of their formation is not known although it likely occurred during a period when meltwater was available at the base of the ice sheet, perhaps during deglaciation (cf. Ó Cofaigh et al., 2002). The channels and depressions are similar in appearance and have similar geometries to crescentic scours and sinuous channels around bedrock peaks in other submarine glaciated terrains (e.g. Graham and Hogan, in press).

3.2. Acoustic facies

Profiles acquired with the TOPAS sub-bottom profiler show that four distinct acoustic facies are present in Disko Trough (Fig. 5). Maximum penetration through the sediment package was 40–50 m. Each of the acoustic facies (AF1- AF4) is described below followed by the interpretation of their depositional setting.

3.2.1. Description

Acoustic facies 1 (AF1) is found at the seafloor on the outer shelf in Disko Trough and mantling bedrock highs on the inner shelf. It comprises a thin (<10 m) acoustically-homogenous unit that conformably drapes underlying units except on steep slopes where this facies disappears. AF2 is also conformable but it is acoustically-

Fig. 4. (a) Multibeam-bathymetric shaded relief image of inner Disko Trough showing areas of rugged seafloor with channels (white arrows) landward of basalt scarps, streamlined glacial landforms, the E-W trending deepest part of the trough, and relevant core locations. Bathymetric contour interval is 50 m. The locations of Fig. 4b, c, and the inset are also shown. Inset shows a seafloor profile over MSGL and sedimentary tails of crag-and tails (arrowed) in the inner trough. (b) TOPAS sub-bottom profile over rugged seafloor and the VC24 core site. At the seafloor is 5–15 m of acoustically-stratified conformable sediment overlying an impenetrable reflection taken to be the surface of the basalt basement in this area. (c) TOPAS sub-bottom profile over subglacial crag-and-tail landforms indicating ice flow from east to west in the trough. 50 m of acoustically-transparent basin fill occurs in the deepest part of the trough.

stratified with individual strata being 1–3 m thick (although thinner strata may present but are below the resolution of TOPAS); the total thickness of this unit ranges from 5 to 20 m. It is present in the deeper E-W trending part of inner Disko Trough (cf. Fig. 5a) and

mantling the adjacent rugged basalt highs. AF3 is acoustically ho-mogenous with a moderate to strong, upper reflection that can be prolonged. This unit has variable thickness in Disko Trough tapering to nothing, infilling local depressions (Fig. 5c), and forming
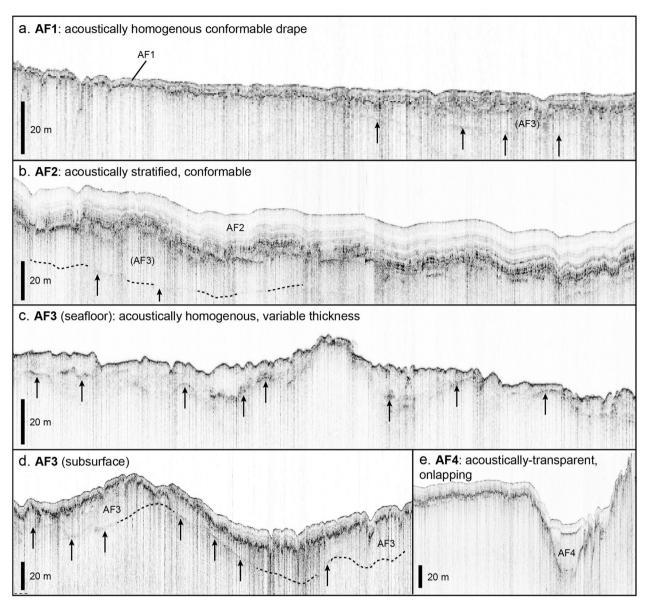
Fig. 5. Examples of the four acoustic facies (AF1-AF4) observed on TOPAS sub-bottom profiles in Disko Trough. (a) AF1: post-glacial hemipelagic/distal glacimarine drape. (b) AF2: deglacial rainout of suspended sediment and IRD. (c) AF3: subglacial till at the seafloor. (d) AF3: subglacial till facies in the subsurface. (e) AF4: local basin fill. The base of AF3, a faint, discontinuous reflection, is arrowed.

positive-relief wedges. Its basal reflection is discontinuous and typically only weak to moderate in strength. AF3 is found at the seafloor on the basalt escarpment where its upper surface is interrupted by iceberg ploughmarks (Fig. 5c). This facies is also found in the subsurface of middle-outer Disko Trough where it is overlain by AF1 and AF2 (Fig. 5b, d); thicknesses range from 0 to 30 m. The GZWs and glacial lineations (tails of crag-and-tails), which are interpreted as landforms formed subglacially, comprise AF3. AF4 is rare in Disko Trough, occurring only where it infills the E-W deep on the inner shelf (Fig. 5e). It is acoustically transparent and onlaps on to the walls of the depression.

3.2.2. Interpretation

The conformable geometry of AF1, its position at the top of the acoustic stratigraphy in Disko Trough, and comparison with other glaciated continental shelf settings is consistent with the interpretation of this facies as a post-glacial drape facies deposited by rainout of sediment in a hemipelagic or distal glacimarine setting

(e.g. Kleiber et al., 2000; Hogan et al., 2012). The distribution of AF2 is limited to the inner part of Disko Trough and this facies was sampled by cores VC01, VC25, VC23 and VC24. The upper strata of AF2 correspond to the post-glacial massive mud facies in cores VC01 and VC25. In VC23 and VC24, which sampled thinner accumulations of AF2, this stratified facies represents the mud-diamicton units with acoustic reflections between strata presumably corresponding to sub-units with different acoustic properties although it is not possible to correlate specific reflections to core properties with the data available. The mud-diamicton units were interpreted as ice-proximal glacimarine deposits (see Section 3.1.3) and their stratified but conformable nature on sub-bottom profiles is consistent with the deposition of material from suspension (from turbid meltwater plumes) and normal rainout (IRD) processes in glacimarine environments (cf. Hogan et al., 2012). The absence of acoustically-transparent wedges interleaved with stratified reflections suggests that downslope resedimentation was uncommon in inner Disko Trough. Having said this, the occurrence of AF4 in a

localised depression only, and its onlapping geometry suggests that this facies consists of material that was focussed into the depression by small-scale slope failures and (or) bottom currents. The unconformable nature of AF3, its varying thickness, and the correlation of this acoustic facies with subglacial landforms (lineations, GZWs) strongly suggest that this acoustic facies represents diamictic material or till deposited in subglacial or proglacial environments (e.g. Ó Cofaigh et al., 2005; Evans et al., 2005). The strong upper reflection of this facies and its acoustically-homogenous character are consistent with the interpretation of AF3 as a till, whereby the mixture of grain sizes scatter acoustic energy and the lack of internal structure result in an acoustically-homogeneous response on sub-bottom profiles.

3.3. Core lithofacies and sediment accumulation rates

Lithological logs, physical parameter data and IRD counts for cores VC 15, VC17, VC19, VC20, VC21, VC26, VC01, VC25, VC23, and VC24 are presented in Fig. 6; example x-radiographs of the lithofacies are given in Fig. 7.

3.3.1. Facies 1: diamictons
3.3.1.1. Description. At the base of the cores VC17 and VC19 is a dark grey (5Y 3/1 to 5Y 4/1) stiff diamicton with a muddy matrix supporting a mixture of sand-, gravel- and pebble-sized grains (Fig. 6a). In VC20 the diamicton unit is found between 425 and 520 cm, 19 cm above the base of the core. The diamicton units are generally massive, except for in VC20 where planar discontinuities can be seen on x-radiographs (after Ó Cofaigh et al., 2013a). Contacts with the overlying units are inclined and sharp to relatively sharp in nature. Gravel- and pebble-sized clasts are subangular to subrounded in shape and consist of one of five lithologies: quartzite, granitoid, carbonate, basalt, and a metamorphosed, amphibole-bearing lithology. Clasts are typically 0.3–2 cm in length. Shear-strength measurements from the diamictons range from high (40–80 kPa) in VC20 and VC17 to moderate to low in VC19 (5–15 kPa). A thin section of the diamicton in VC17 at 61–70 cm core-depth reveals sinuous discontinuous cracks in areas of fine-grained matrix and discrete clusters of sand-sized grains or steeply-inclined clasts; turbate structures and shell fragments are rare, and foraminifera are absent. The MS of the diamicton in VC20 is generally low ($20–300 \times 10^{-5}$ SI) and varies from sharp peaks to troughs (Fig. 7).

3.3.1.2. Interpretation. On the basis of the high shear strength of the diamicton in VC20, and on the presence of asymmetric deformation structures (parallel fractures, fractured grains turbate structures, lineaments) indicating shear, in a thin section from this unit, Ó Cofaigh et al. (2013a) interpreted this diamicton as a subglacial till; this interpretation is maintained here. The variability in the MS probably reflects the changeable grain size of the unit and the fairly low values when compared with overlying units (Fig. 6a) may indicate that the diamicton contains few basaltic clasts because ferromagnetic minerals in basalts retain strong magnetic signatures. The micro-structure of the diamicton in VC17 coupled with its lower shear strength values lead to the interpretation that this unit is a glacimarine diamicton deposited in an ice-proximal setting either as subglacial material emanating from, but deposited in front of, the grounding line, or as an iceberg-rafted deposit. The presence of discrete clusters of grains and deformation at the base of these clusters at the micro-scale indicate an origin as an iceberg-rafted diamicton is most likely; highly inclined to vertical clast orientations observed in the thin section support this interpretation. The low shear strength measurements of the diamicton in VC19 and VC15 together with the similarity of these units with

the diamicton in VC17 suggests that the VC19 and VC15 diamictons can also be interpreted as an iceberg-rafted glacimarine diamictons.

3.3.2. Facies 2: muddy sands with pebbles/muddy sands
3.3.2.1. Description. At the base of VC21 and overlying the diamictons in VC17, VC19, and VC20 are grey-brown (5Y 5/1 to 5Y 5/2), fine to medium, poorly-sorted sand units containing occasional gravel layers and dispersed outsized clasts. Thicknesses of this unit are less than 40 cm in all cores where present; in VC19, our outermost shelf core site, this unit is only 8 cm thick. From visual inspection of the cores the facies appears mostly massive, however x-radiographs reveal that the sands are occasionally weakly-to-moderately-laminated to stratified with occasional planar discontinuities (Fig. 8b), and patches of finer-grained material and gravel layers (Fig. 8a). In VC21 the unit is moderately-stratified with 2–3 cm thick strata, clast-rich layers and a possible load structure at 486–488 cm core-depth (Fig. 8b). Dispersed or clustered clasts in this unit are subangular to subrounded in shape and are typically between 0.3 and 1.2 cm in length; quartzite, carbonate, granite, and basalt lithologies occur. The clasts show moderate alignment that is parallel to the planar discontinuities in the core. Counts of clasts >2 mm are moderate to high (4–30 clasts per 2 cm window) but variable in outer shelf cores (VC15, VC17, VC19, VC20); in VC21 the clast content is typically lower (<5 clasts per 2 cm window) (Fig. 8a). Investigations of the microfauna in VC21 indicate that this facies is barren or contains rare, poorly-preserved tests of *Islandiella helenae* and *Cibicides lobatulus*. In VC20 the muddy sands are dominated by *I. helenae* but also includes *Cassidulina reniforme* and *Elphidium excavatum* f. *clavata* (Jennings et al., 2013).

The shear strength of the muddy sands is moderate with measurements between 10 and 20 kPa in VC19 and VC20 (Fig. 8a). MS data is only available for VC20 where the values are inconsistent varying between peaks and troughs, and only showing weak correlation with grain size in the unit above the diamicton (Fig. 7a). There, MS values appear to be slightly lower in the coarser-grained facies. In general, MS values appear to be higher in the sands above the diamicton (397–422 cm) than those underlying the diamicton (520–539 cm).

3.3.2.2. Interpretation. The up-core transition from diamicton to pebble-rich muddy sands in outer Disko Trough cores (VC15, VC17, VC19, VC20) marks a change in depositional environment from subglacial (VC20) or adjacent to the grounding line (VC17, VC19, VC15) to a location slightly more distal from the ice-stream margin, although still ice proximal. The high clast content and distinct gravel layers and clusters indicate that iceberg rafting was an important process and stratification confirms subaqueous deposition. This unit is interpreted as ice-proximal coarse-grained sediment originating as basal debris from the nearby grounding line (cf. Domack et al., 1999) with additional IRD deposition. The same clast lithologies occur in this facies as were found in the diamictons because both are derived largely from the basal debris zone. The moderate shear strength of Facies 2 reflects compaction and dewatering of this coarse-grained lithofacies by overlying sediments, and the up-core transition from Facies 2 to the overlying fine-grained muds with outsized clasts indicates retreat of the grounding line away from the core sites.

The foraminiferal assemblages of the sandy units are an indicator for cold conditions associated with the marginal sea-ice zone (Polyak and Solheim, 1994; Jennings et al., 2013), and for core VC20 Jennings et al. (2013) interpreted this unit to have been deposited during retreat of the ice margin via calving with the setting changing rapidly from ice proximal to ice distal from c. 12.2 to 11.4 cal kyrs BP. We note that 12.2 cal kyrs BP is a maximum age for
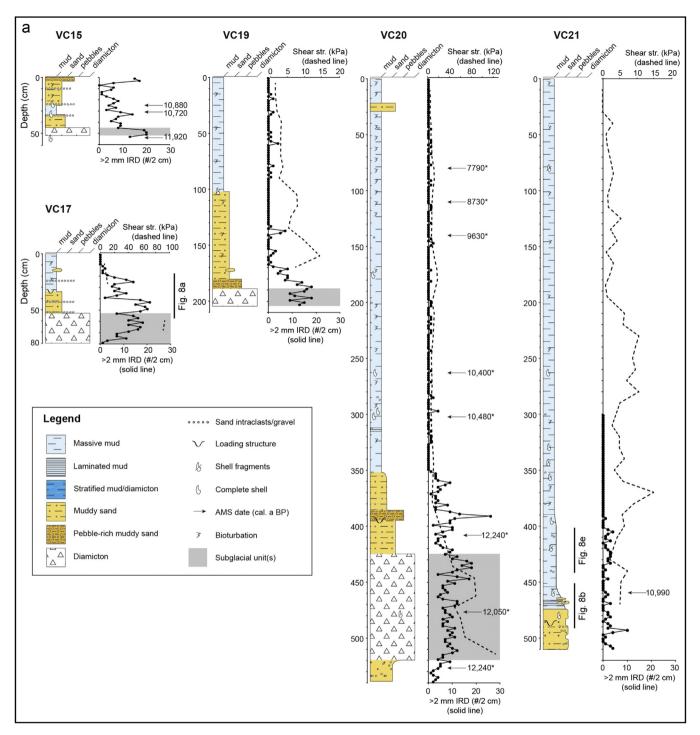
Fig. 6. a. Sedimentary lithofacies logs, ice-rafted debris (IRD) counts, shear strength (shear str.; for all except VC15), and calibrated AMS radiocarbon dates for cores from outer Disko Trough. Note the different scales on the shear strength plots. Sedimentary logs for VC15 and VC20 and dates marked with an asterisk (*) were reported previously by Ó Cofaigh et al. (2013a); IRD counts for VC20 from Jennings et al. (2013). The positions of x-radiographs shown in Fig. 5 are also shown. Core logs are displayed in order across the West Greenland shelf from the shelf break; see Fig. 2 for core locations. b. Sedimentary lithofacies logs, ice-rafted debris (IRD) counts (VC24 only), shear strength (shear str.; for all except VC01), and calibrated AMS radiocarbon dates for cores from inner Disko Trough. Note the different scales on the shear strength plots. The positions of x-radiographs shown in Fig. 5 are also shown.

this unit because it is derived from a shell reworked in to this unit from the underlying till and so dates the readvance of ice on to the outer shelf (Ó Cofaigh et al., 2013a). A date of 11.0 cal kyrs BP from 10 cm above the sandy unit in VC21 (Table 2; Fig. 3a) is consistent with the chronology for retreat in outer Disko Trough but does not further constrain rapid retreat from the outer shelf.

3.3.3. Facies 3: stratified muds and diamictons

3.3.3.1. Description. At the base of cores VC23 and VC24 are thick sequences (up to 200 cm) of stratified grey muds and grey-brown diamictons or sands with outsized clasts, occasional sand lenses, and rare shell fragments (Fig. 6b). The grey sub-units (5Y 5/1 to GLEY 6/1) consist of fine-grained muds with some dispersed clasts;
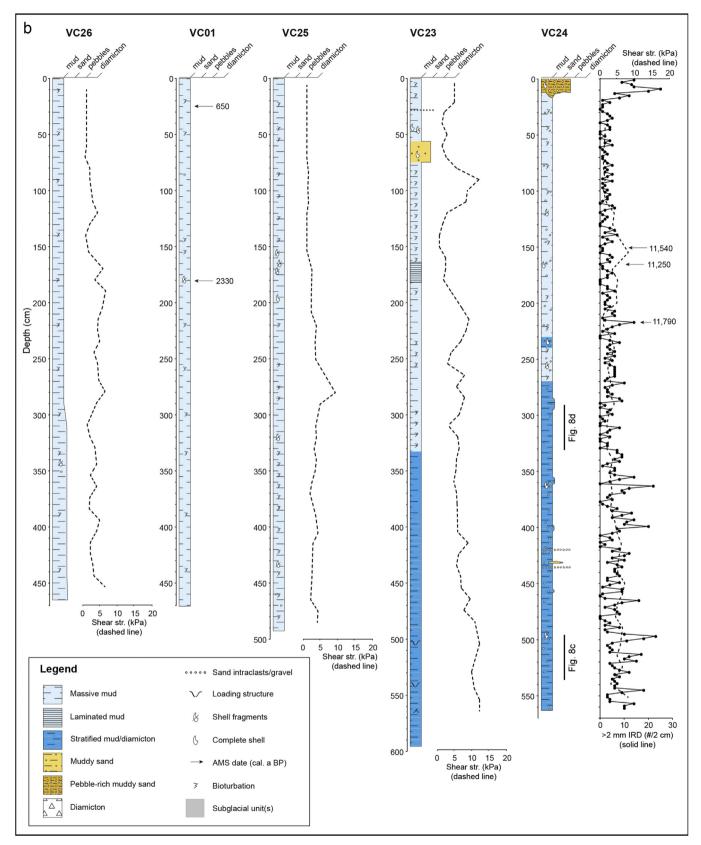
Fig. 6. (continued).

the brown-grey (2.5Y 5/2) sub-units consist of a higher proportion of silt- and sand-sized grains and a high content of dispersed clasts and can be classified as diamictons. The diamicton units are typically thicker (1—3 cm) than the finer-grained units (<1 cm) (Fig. 8c);
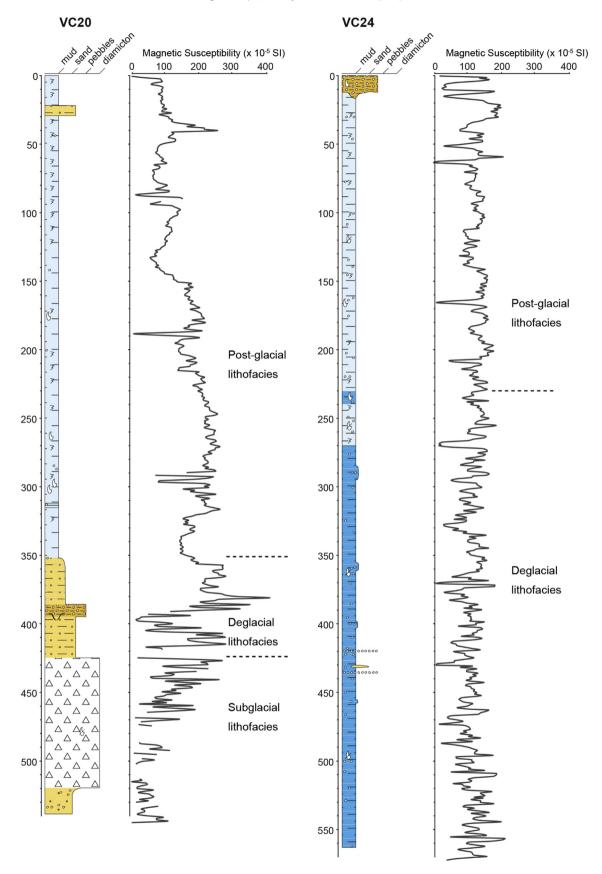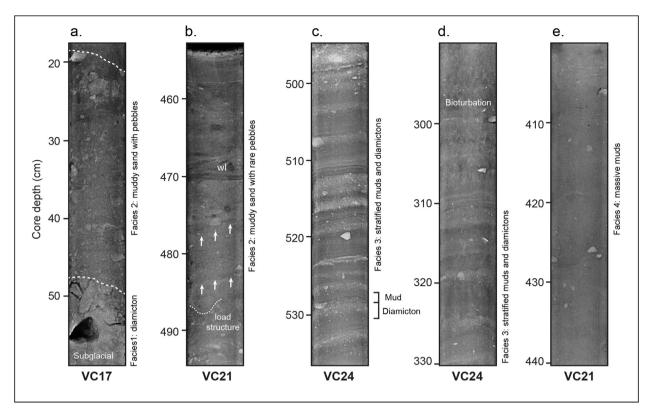
Fig. 7. Magnetic susceptibility (MS, SI: International System of Units) for core VC20 on the outer shelf and core VC24 on the inner shelf of Disko Trough.

Fig. 8. X-radiographs of sedimentary lithofacies from Disko Trough cores. (a) 18–58 cm core-depth in VC17 showing basal diamicton with diffuse transition to pebble-rich muddy sand and an change to massive muds at the top of the image. (b) 454–494 cm core-depth in VC21 showing muddy sands with occasional pebbles, faint wispy laminations (wl), and planar discontinuities (arrowed). (c) 496–536 cm core-depth in VC24 showing well-defined alternating strata of muds with rare outsized clasts and diamictons; boundaries between the strata vary from sharp to diffuse. (d) 291–330 cm core-depth in VC24 showing the upper part of the stratified mud-diamicton facies with more diffuse boundaries between the strata and bioturbation from 291 to 308 cm core-depth. (e) 401–440 cm core-depth in VC21 showing the uppermost lithofacies in the Disko Trough cores, massive muds with occasional outsized clasts and shells.

clasts are largely restricted to the diamicton layers. The clasts are subangular to subrounded and are up to 3 cm in length; clast lithologies are dominantly granite and basalt. Contacts between the coarser- and finer-grained sub-units are horizontal to subhorizontal, and appear diffuse or gradational on visual inspection of the core. However, x-radiographs of VC24 reveal that the contacts vary from diffuse to sharp (Fig. 8c), and that they are sometimes deformed by load structures or localised faulting. In general, the upper contacts of the diamicton units are sharp whereas their lower contacts are more diffuse or gradational. There is a down-unit trend to better-defined strata with sharper contacts between the sub-units. From 510 cm to the base of the core the finer-grained mud units are laminated and contain coarser 0.1–0.3 cm thick laminae that are sometimes only weakly defined. From 270 cm to 310 cm core depth the unit is bioturbated and vertical burrows have "smeared" or destroyed the mud-diamicton boundaries in patches. In total, there are at least 74 mud-diamicton pairs or "couplets" from 310 cm to the base of the core that can be seen on the x-radiographs.

IRD counts from this unit (Fig. 6b) reveal the variable clast content of the mud and diamicton units as distinct peaks and troughs of IRD; 24 distinct IRD peaks can be counted from 310 cm to the base of the core. Slightly increased IRD contents are apparent in the x-radiographs and IRD count data at 490–525 cm core-depth corresponding to higher clast contents in the diamicton sub-units in this interval. Foraminifera tests are rare throughout Facies 3 but some tests of *Cassidulina reniforme* occur in the uppermost 50 cm; *S. biformis*, *S. feylingi* and *E. excavatum* occur between 350 and 400 cm. The MS of the stratified muds varies between about 50

and 200×10^{-5} SI (Fig. 7) and is characterised by 66 distinct peaks from 310 cm to the base of the core (above 310 cm this facies is bioturbated).

Interpretation: The deposition of alternating diamicton and laminated to massive mud units with rare clasts results from switches between glacimarine sedimentation processes during ice retreat in Disko Trough. The diamicton units represent sedimentation predominantly from iceberg rafting, as well as suspension settling of finer grains. The massive to laminated mud facies, however, was deposited when iceberg rafting was overwhelmed by meltwater and fine-grained sediment supply to the trough as is indicated by the very low clast contents. In East Greenland such mud units, when alternating with iceberg-rafted diamictons, have been interpreted as the product of suspension settling during periods with extensive sea-ice cover that prevented iceberg drift over the area (Jennings and Weiner, 1996; Dowdeswell et al., 2000; Smith and Andrews, 2000). In Alaska, such mud-diamicton couplets reflect seasonal switching between sedimentation dominated by settling from turbid meltwater plumes (muds) in summer months and sedimentation from icebergs (diamictons) calved in winter (Cowan et al., 1997; Cai et al., 1997; Ullrich et al., 2009). Although there is some evidence, based on dinocyst proxy data, for near perennial sea-ice cover on the outer shelf in Disko Trough during retreat (Jennings et al., 2013), the occurrence of some large clasts (IRD) in the mud units indicates that icebergs were still passing over the area during the deposition of this facies. In addition, although foraminifera are rare in the stratified unit, the faunal assemblage is associated with modern glacimarine settings (cf. Schafer and Cole, 1986; Jennings and Helgadóttir, 1994), and

indicates that turbid meltwater was present during deposition. Thus, we prefer a meltwater origin for the muds with occasional icebergs, over periods of complete sea-ice cover. Facies 3 is interpreted as the product of alternating sedimentation from icebergs and from turbid, subglacially-derived meltwaters with the dominant depositional process varying over time.

In the upper part of the mud-diamicton unit in VC24 the diamictons are less well-defined and contain fewer gravel-sized clasts (Fig. 7d) and this is interpreted to represent a gradual increase in the importance of sedimentation from suspension over iceberg calving with time possibly related to ameliorating climatic conditions and, therefore, increased ice-mass loss by melting rather than calving. The occurrence of bioturbation, which becomes extensive towards the top of this unit, also supports ameliorating conditions and retreat of the ice margin further landwards (to the east) during the deposition of these units.

3.3.4. Facies 4: massive to laminated muds

3.3.4.1. Description. The upper 33–455 cm of all of the studied cores in Disko Trough, apart from VC15 on the outermost shelf, consists of green-grey to grey massive muds (5Y 4/3 to 5Y 4/1); cores VC01 and VC25 only sampled this unit (Fig. 6b). The muds are heavily bioturbated sometimes with black mottles on their surface, and contain mollusc shells or shelly fragments. They contain only rare outsized clasts and sand-sized grains (Fig. 8e) and are very soft with high water contents; shear-strength measurements are typically less than 5 kPa and free-standing water was present during core logging. MS (based on data from VC01, VC20 and VC24) varies from 10 to 250 $\times$ 10^{-5} SI with down-core trends varying from increasing (VC20), to decreasing (VC01; not shown) to remaining roughly consistent with multiple peaks and troughs (VC24) (Fig. 7). Noted clast lithologies are carbonates and granites.

A full foraminiferal analysis was conducted on VC20 by Jennings et al. (2013) who found that the homogeneous grey-green muds were dominated by agglutinated taxa at their base, including a species indicative of cold conditions and glacial meltwater (*Spiroplectammina biformis*), and a cold-water species, *Cuneata arctica*. Calcareous foraminifera, which occur at discrete intervals, were dominated by *Islandiella norcrossi* which is an arctic species indicative of WGC Atlantic water and low amounts of glacial meltwater in Disko Bugt (Lloyd et al., 2005; Perner et al., 2012). At the top of the core warmer water agglutinated forams occur and few carbonate tests suggest poor carbonate preservation in low accumulation rate sediments (Jennings et al., 2013). Evidence from the remaining cores, apart from VC17 which appears to be barren of foraminifera, indicate a similar pattern of agglutinated forams and carbonate tests including *I. helenae*, *Nonionella labradorica*, *E. excavatum* and *C. reniforme* in the lower parts of the muds. Up-core more tests of *I. norcrossi* and *N. labradorica* occur, along with the other Arctic taxa. Radiocarbon dates from the upper 2 m of this facies in VC01 (Table 2) return young ages of less than 2500 cal yrs BP.

3.3.4.2. Interpretation. The homogeneous, bioturbated grey-green muds are interpreted as hemipelagic post-glacial sediments deposited from suspension in an open-marine setting with occasional deposition from icebergs. The post-LGM age of the muds Jennings et al., 2013 is supported by the new dates from VC01. The foraminiferal assemblages of the muds indicate a transition from cold conditions and the marginal sea-ice zone at their base, to warmer waters and the influence of Atlantic water in the trough. This is consistent with palaeoceanographic records from the inner shelf and Disko Bugt showing that the influence of the WGC only increased after ca. 9.2 ka (Lloyd et al., 2005; McCarthy, 2011). The disappearance of carbonate tests in the uppermost parts of the

muds are taken to reflect poor carbonate preservation after Jennings et al., 2013. The presence of carbonate IRD indicates that icebergs from northern Baffin Bay (Andrews and Eberl, 2011) have drifted over Disko Trough during the deposition of this post-glacial mud facies (cf. Jennings et al., 2013).

3.3.5. Sediment accumulation rates

The new radiocarbon dates presented here (Table 2) along with previously-published deglacial ages from Disko Trough allow for the calculation of average sedimentation rates for the deglacial lithofacies in VC21 and VC24. Grounded ice retreated from the VC21 core site sometime shortly after 12.24 cal kyr BP because it is known that ice retreated from VC20 only 6 km further west after by this time (Ó Cofaigh et al., 2013a). Consequently, 12.24 cal kyr BP can be taken as an assumed basal date for VC21. The date of 10.99 cal kyr BP from 460 cm core-depth in VC21 (Table 2; Fig. 3a) is just above the transition to postglacial muds in the core resulting in an average sedimentation rate for the deglacial unit of 0.04 cm a^{-1}. For VC24, we can use established regional chronology and a tie point with core MSM343340, which is located at the same longitude as VC24 but is 3 km north of the multibeam data coverage (Figs. 2 and 4) to constrain the time period during which deglacial sediments accumulated. Ice-retreat from the outer shelf occurred after 12.2 cal kyr BP (Ó Cofaigh et al., 2013a), and the deepest radiocarbon date in MSM343340 (12.1 cal kyr BP) has been tied to a depth of 280 cm in VC24, which is near the top of the deglacial sediment unit, by comparing foraminiferal faunas (Perner and Jennings, pers. comm., 2015). Thus, these two dates approximately constrain the age of the stratified, deglacial unit and return an average sedimentation rate for this unit of 2.8 cm a^{-1}. Dates from 217 to 218 cm and 165 cm core-depth in the postglacial mud facies in VC24 (Table 2) give an average sedimentation rate for the lower part of this unit of 0.1 cm a^{-1}.
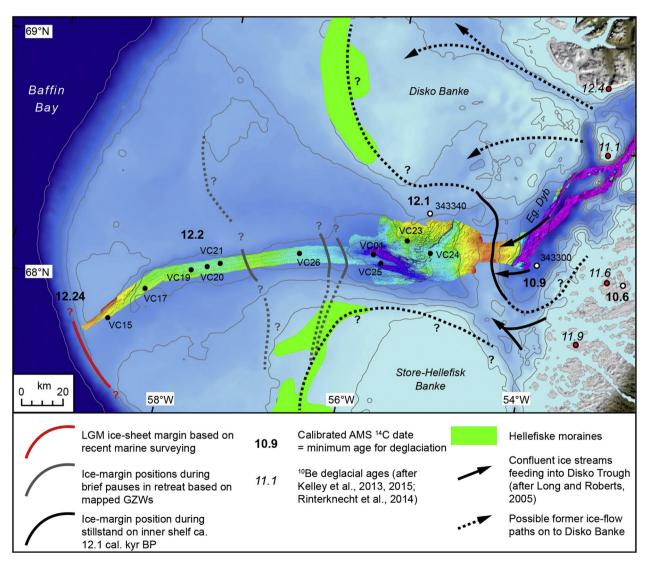
4. Discussion

4.1. Ice-stream retreat and configuration in Disko trough

The deglacial lithofacies and IRD counts from vibrocores VC15-VC21 is consistent with rapid ice-stream retreat across the outer shelf after the Younger Dryas readvance to the shelf edge at c. 12.24 cal kyr BP (Ó Cofaigh et al., 2013a; Rinterknecht et al., 2014). The thin, sandy units with abundant IRD (Facies 2) suggest that the cores were located proximal to the ice margin, at one time during overall retreat from the outer shelf, and that the main mechanism for initial ice loss was calving of icebergs. The up-unit decrease in IRD content in these units (Fig. 6a) most likely shows that the ice margin was retreating further eastward during the deposition of these units and, as a result, fewer icebergs passed over the core sites or the majority of the debris had already melted out of the bergs by the time they drifted across the outer shelf. In addition, the thickness of this deglacial facies increases with distance towards land from the shelf break (Fig. 6a) suggesting that either retreat was most rapid on the outermost shelf and (or) that winnowing of some sediment occurred. Acoustic profiles confirm that there is very little (<5 m) unlithified sediment cover on the outer shelf over a thin sheet of subglacial till with varying thickness. The till unit, which is sampled in the outer shelf cores (VC15, VC17, VC19, VC20), is evidence for grounded ice flow in Disko Trough during the last glacial but the somewhat surprising absence of any glacial landforms on the outer shelf (cf. Fig.2) may support the inference that the Younger Dryas readvance of grounded ice removed sediments related to ice advance and retreat on the outer shelf during the LGM (Ó Cofaigh et al., 2013a).

The rapid initial retreat of ice in Disko Trough over a distance of

around 110 km from VC20 to around 55°18′W, which occurred between 12.24 and 12.08 cal kyr BP (McCarthy, 2011; Ó Cofaigh et al., 2013a) appears to have been punctuated by between 1 and 3 brief stillstand events during the 160 years of retreat across the shelf (Fig. 9) forming the mid-shelf GZWs (Fig. 3). This tight time-frame is indirect evidence for the rate of formation of GZWs, which must have been built up on the order of decades or less in Disko Trough. The middle ridge in Disko Trough (GZW 2 on Fig. 3), which is most confidently interpreted as a GZW, has an estimated volume of 7.95×10^8 m^3. Assuming that the GZW extends across the entire 20 km-wide trough means that a volume of around 39,750 m^3 per metre of trough width has accumulated during the stillstand event. Estimates of the sediment flux at the grounding line of ice streams in West Antarctica today are on the order of 150 m^3 a^{-1} m^{-1} (m^3 per year per metre of ice-stream width) (Anandakrishnan et al., 2007). Using this flux rate the GZW in Disko Trough would have taken 265 years to form. Given that marine radiocarbon dates suggest that retreat through this part of the trough occurred in as little as 160 years this flux rate must be too low for the palaeo-ice stream

occupying the trough. Supposing that near instantaneous retreat of ice occurred in the trough, and that each GZW (3 total) formed in about 50 years, would require flux rates to be at least five times as high as the modern rates i.e., more than 750 m^3 a^{-1} m^{-1}. Such large flux rates are not unreasonable; rates on the order of several hundred cubic metres per year per metre ice stream width have been estimated for sediment volumes deposited at the margins of palaeo-ice streams (Dowdeswell et al., 2008) and hypothesized for subglacial till transport at the base of ice streams (Alley et al., 1986; Tulaczyk et al., 2001; Christoffersen et al., 2010). Moreover, a sediment flux as high as 2030 m^3 a^{-1} m^{-1} was estimated for the Jakobshavns Isbrae when it was located at the mouth of Jakob-shavns Isfjord during deglaciation, with the high flux rate possibly being explained by the narrow geometry (<10 km) of the fjord (Hogan et al., 2012). However, this discussion again highlights the need for better chronological control on GZWs in order to deter-mine their rates of formation and, thus, their relative significance for ice-stream stabilisation during the retreat or large ice masses. Indeed, the brevity of the YD advance and retreat may suggest that

Fig. 9. Reconstruction of ice-margin positions in Disko Trough since the Younger Dryas readvance to the shelf break based on mapped glacial landforms and dated marine sed-iments. Dashed lines indicate conceptual ice-margin positions only. The position of the ice margin during the stillstand on the inner shelf (black) depicts a calving bay over inner Disko Trough; ice margin on the banks follows the 200 m contour approximately and connects with the Hellefiske moraines on the mid-shelf. Outer shelf deglacial ages (calibrated) from Ó Cofaigh et al. (2013a), inner shelf ages from cores MSM343340 and MSM343300 after McCarthy (2011) and Quillman et al. (2009), respectively; terrestrial radiocarbon age from Long and Roberts (2003).

the mid-shelf GZWs were formed during the first retreat of ice from the shelf break, i.e., prior to the YD readvance. However, if correct, these flux rates from the shelf also require relatively thick, grounded ice in Disko Trough during deglaciation in order to deliver this much sediment to the retreating margin. This is somewhat contradictory with modern views on the LGM GrIS which advocate perhaps only thin, lightly grounded outlet glaciers reaching the shelf break in West Greenland (e.g. Roberts et al., 2009, Hofman et al., 2016).

Once ice had retreated landward of the GZWs in Disko Trough, i.e., east of 56°10′ W, the deglacial lithofacies (Facies 3, Fig. 8) and acoustic profiles indicate a switch from rapid retreat with ice loss mostly as icebergs to an ice-proximal environment where the release of meltwater became an important mechanism for mass loss. The deepest date in core MSM343340 just north of our multibeam coverage at 55°20' W (Figs. 1 and 4) was 12.1 cal kyr BP (McCarthy, 2011) and confirms that the ice margin was east of the area of rugged seafloor terrain by this time. Indeed, the deglacial stratified mud-diamicton unit (core Facies 3, AF 2) appears to have been deposited rapidly between 12.2 and c. 12.1 cal kyr BP, at least in VC24 (see Section 3.3.3). The next marine radiocarbon date available is from outer Egedesminde Dyb about 50 km further east and landward of the basalt escarpment that separates Disko Trough from Egedesminde Dyb (Weidick and Bennike, 2007); thus this gives a minimum date for deglaciation to somewhere east of the basalt escarpment by 10.9 cal kyr BP (Fig. 9) (Quillman et al., 2009). However, terrestrial cosmogenic radionuclide (CRN) exposure ages from Nunarssuaq, an island at the eastern end of Egedesminde Dyb, suggest that the island, and therefore the trough, was deglaciated by 11.1 kyr BP (Kelley et al., 2013). As such, the ice margin may have taken as much as ca. 1000 years (12.1—11.1 kyr BP) to retreat over the basalt plateau and escarpment.

Based on the chronology established for the stratified deglacial unit in VC24 (Facies 3, Fig. 8c) these units may have been deposited in as little as 100 years, indicating that stabilisation of the ice on Disko and Store-Hellefiske banks and on the basalt escarpment was probably only for a few hundred years, rather than 1000 years. It is not possible to further constrain the timing of this stillstand from marine data at this time because the existing marine cores do not penetrate the base of the deglacial stratified unit in either Disko Trough or Egedesminde Dyb. However, CRN ages of from the coast just east of Egedesminde Dyb support rapid deposition of the stratified unit as coastal areas were potentially ice-free by 11.9 kyr BP (Kelley et al., 2015, Fig. 9).
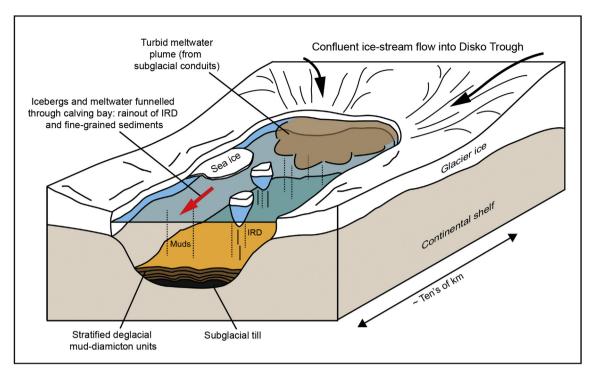
The alternation of diamicton units with laminated muds (core Facies 3, AF2) indicates that, shortly after 12.2 kyr BP, the ice-proximal environment in inner Disko Trough was characterised by periods of iceberg calving and of large influxes of subglacially-derived turbid meltwaters, and that deglacial sediments accumulated over the rugged seafloor terrain (Fig. 4b, c). Assuming that the ice margin was indeed stabilised on the shallow banks and basalt escarpment during this slowdown in retreat, or even on land southeast of Egedesminde Dyb after Kelley et al. (2015), then it seems likely that the inner trough was "surrounded" by grounded ice and that a calving bay (Fig. 10), through which meltwater and icebergs were expelled, existed in inner Disko Trough sometime between c. 12.2 and 11.1 cal kyr BP. Presumably icebergs, meltwater and sediment were channelled primarily through the deep, WNW-ESE trending trough in the southern part of the trough (LGM water depths >480 m; Figs. 4a and 9). Indirect support for this comes from sub-bottom profiles showing that the deeper, southern part of the trough contains the thickest deglacial and postglacial sediments (up to 20 m of AF1 and AF2) whereas the basalt surfaces are typically mantled with less than 5—8 m of sediment above a thin till unit. However, basin infill and onlapping at the sides of the deep

indicates that the redeposition of material from steep sidewalls contributed to the enhanced sediment thicknesses (AF4, Fig. 5e) (cf. Hogan et al., 2012).

4.2. Deglacial lithofacies as indicators of style of ice-stream retreat in Disko Trough

The limited thickness of deglacial lithofacies on the outer to middle shelf (Fig. 6a), and their formation as units deposited from the rainout of IRD, indicates that the rapid retreat across the shelf was driven largely by calving rather than melting. Evidence from palaeoenvironmental proxies in VC20 and in cores acquired beyond the shelf break also support rapid ice retreat via calving on the outer shelf Jennings et al., 2013. It is interesting to note that there does not appear to be a change in the deglacial lithofacies sampled from cores acquired on the outer shelf to VC21 which acquired sediments from immediately seaward of the largest GZW (see Fig. 3a) where the ice margin must have paused, at least for a time, during retreat. We acknowledge, however, that the deglacial lithofacies may be thicker or more variable close to the GZWs than we have described here but that the vibrocorer did not recover these sediments (VC21 bottoms out in an IRD-rich deglacial unit and VC26 contains only post-glacial muds; Fig. 6b). Alternatively, deglacial units from the first retreat from the outer shelf were removed during the YD readvancing ice sheet (cf. Ó Cofaigh et al., 2013a). Thus, we tentatively conclude that the dominant mechanism of ice loss remained the calving of icebergs during this final, rapid retreat phase across the mid-shelf.

A major change in the style of retreat, and the mechanisms of ice-mass loss, occurred when the ice margin was located on the inner shelf around 12.2—12.1 cal kyr BP. At this time ice retreat was punctuated by a major stillstand when the ice margin was likely stabilised on the shallow banks on either side of the trough and on the basalt escarpment at the head of Disko Trough, possibly leading to the formation of a calving bay (see above discussion; Figs. 9 and 10). Presumably, the abrupt temperature rise at the start of the Holocene chron at 11.7 ka BP (Dahl-Jensen et al., 1998; Rasmussen et al., 2006) led to high rates of melting and thinning at the ice-sheet margin which increased meltwater and sediment supply to the marine environment. The meltwater flux that resulted from increased temperatures may have been complimented by increased basal melting from the grounded ice margins around the head of the trough as the ice would have had to overcome the shallow, rugged banks in order to drain through the trough. Ice flow over the rough, shallow banks would have caused enhanced basal melting due to increased pressure on the upstream sides of the topographic highs and obstacles at the bed.

The deglacial lithofacies (core Facies 3, AF2) from cores acquired on shallower bedrock areas in the trough (VC23-24; Figs. 4a and 9) show that sedimentation from meltwater plumes was a major depositional process at this time and that sedimentation from turbid meltwaters likely overwhelmed the deposition of IRD periodically. The estimate of the average sediment accumulation rate for this unit (2.8 cm a^{-1}) is two orders of magnitude greater than that calculated for the IRD-dominated units on the outer shelf in VC21 (0.04 cm a^{-1}) and VC20 (0.05 cm a^{-1}; Jennings et al., 2013). However, this accumulation rate is much lower than rates of several tens of centimetres per year for mud-diamicton couplets described from Alaskan fjords that are interpreted as strongly seasonal in nature, i.e., glacimarine varves (Cowan et al., 1997; Cai et al., 1997; Ullrich et al., 2009). Using the approximate chronology for the mud-diamicton unit in VC24 (deposited over c. 100 years) and the number of couplets identified in that core from x-radiographs (74) we can calculate an average cyclicity of around 1.3 years for the deposition of each couplet. This is close to being an annual signal

Fig. 10. Schematic model of the calving bay in inner Disko Trough during a major stillstand in ice retreat (not to scale). The ice margin is grounded on the basalt escarpment and shallow banks flanking the trough; icebergs and meltwater (plumes) are funnelled through the embayment. Intermittantly sea-ice cover is complete in the leading to the deposition of fine-grained muds, alternating with periods with reduced sea-ice cover when icebergs can exit the bay (as drawn) depositing a diamicton deglacial facies.

especially if we consider that some couplets may be difficult to distinguish visually from x-radiographs if they are particularly thin or absent in colder years with low meltwater basal flux, for example. Therefore, the rhythmicity in the lithofacies could reflect a seasonal response with increased melting in the summer months leading to deposition of fine-grained muds followed by IRD-dominated deposition in winter months when calving is the mode of mass loss. This is similar to the glacimarine varves described from southern Alaskan fjords today, although sedimentation rates are much lower. This probably relates to the difference in climate between temperate Alaskan glacimarine settings which are heavily-influenced by meltwater (cf. Domack and McClennan, 1996; Gilbert, 2000) and the subpolar or polar environments on that probably existed in West Greenland during deglaciation, even during the Younger Dryas chron which still had warm summers in southern Greenland (cf. Björck et al., 2002).

To our knowledge, this is the first time that stratified, possibly seasonal, mud-diamicton units (core Facies 3) have been described from a continental shelf setting; the examples from Alaska all occur in fjord settings less than 16 km from the calving glacier margin (Cowan et al., 1997). Interestingly, a thin unit (<30 cm) of stratified muds and diamictons also occurs in one core from the inner shelf in Uummannaq Trough (Sheldon et al., 2016) about 250 km north of Disko Trough. This suggests that alternating meltwater- and IRD-dominated deposition also occurred in Uummannaq Trough during retreat sometime before 10.8 cal kyr BP (Sheldon et al., 2016). In East Greenland, the stratified mud-diamicton units were found in fjord or fjord-mouth (coastal) environments, where shorefast sea ice could form. Presumably the occurrence of thick (>200 cm) mud-diamicton units on the continental shelf in Disko Trough is related to the confined ice-margin configuration that focussed glacial meltwater and icebergs, and thus deglacial sedimentation, in to inner Disko Trough. This unique ice-margin configuration (i.e. calving bay, Fig. 10) plus an increase in meltwater supply during a stillsand event led to the deposition of the mud-diamicton lithofacies on the inner shelf. In contrast, on the outer shelfretreat occurred primarily by iceberg calving forming the sandy, clast-rich deglacial lithofacies.

4.3. Regional significance

The GZWs in Disko Trough identified here are significant in terms of the regional pattern of ice-sheet retreat in West Greenland. In addition to the GZWs in Disko Trough, large mid-shelf GZWs have also been identified in Uummannaq Trough 250 km to the north (Dowdeswell et al., 2014), and in Fiskanæs Trough 650 km to the south (Ryan et al., in press). A bathymetric shallowing that could be a large GZW can also be seen extending across the Holsteinsborg Dyb cross-shelf trough at 66°N in the regional bathymetry (IBCAO v. 3.0; Jakobsson et al., 2012). Similar to Disko Trough, the large GZW in Uummannaq Trough occurs on the cusp of a section of trough with a landward slope but the GZW has a more classic wedge-shaped cross profile (see Fig. 10 in Dowdeswell et al., 2014); in Fiskanæs Trough the GZW, which is several tens of metres high and about 10 km wide, occurs entirely on a reverse-bed slope. The presence of several large GZWs in cross-shelf troughs over a stretch of continental shelf at least 900 km long is perhaps suggestive of a regional ice-sheet stabilisation during deglaciation. Alternatively, it could indicate local topographic effects promoting stabilisation of individual ice streams at different times during retreat. We know from marine dates from Uummannaq Trough and trough-mouth fan (Ó Cofaigh et al., 2013a; Sheldon et al., 2016), along with CRN ages and terrestrial geomorphological evidence onshore of Hosteinsborg Dyb (Roberts et al., 2009) that ice extended to the mid-outer shelf in both these troughs during the LGM. In Uummannaq Trough, local topographic effects appear to be limited as the trough is wide (>50 km) along its length and has a very straight axis, although several bathymetric shallowings do

occur on the outer shelf (Sheldon et al., 2016). Fiskanæs and Holsteinsborg troughs also have straight axes. At present, the detailed chronology of ice-sheet retreat in West Greenland is not known well enough to be able to correlate these glacial landforms over the region but existing dates and reconstructions for the GrIS during deglaciation do not point toward synchronous responses of the ice sheet on the shelf (Ó Cofaigh et al., 2013a; Sheldon et al., 2016), although retreat on the inner shelf of West Greenland may have been broadly coherent (e.g. Roberts et al., 2009).

The deglaciation of Disko Trough is known to have been somewhat different from retreat in the Uummannaq system. For example, a YD readvance is only known from Disko Trough to date, after which the outlet in this trough retreated across the shelf almost instantaneously. In contrast, ice in Uummannaq Trough likely paused on the mid-shelf for much of the YD (Sheldon et al., 2016). Marine dates suggest that ice in Disko Trough was located on the inner shelf (close to the basalt escarpment) by c. 12.2 cal kyr BP where it may have remained for some time (Fig. 9; Rinterknecht et al., 2014). However, new CRN ages at the coast and on Disko Ejland indicate either that the ice margin was on land, or perhaps more likely, extensive ice-sheet thinning occurred here very shortly afterward (Fig. 9; Kelley et al., 2013; 2015; Rinterknecht et al., 2014). A discussion of the thinning history of the western GrIS is beyond the scope of this paper but the occurrence of deglacial (proximal) facies on the inner shelf being deposited at 12.2–12.1 kyr BP confirms that at least the Disko outlet glacier remained in the trough delivering large volumes of sediment and meltwater to Disko Trough even whilst the surrounding ice sheet thinned significantly. At this time the ice margin may have been stabilised on one or both of the shallow banks flanking the trough (Fig. 9). Rinterknecht et al. (2014) explained the residual ice in the trough with concurrent major thinning by suggesting that the outlet glacier had a shallow surface profile beyond the basalt sill, with low basal shear stresses and subglacial meltwater facilitating flow across the shelf. Our landform evidence of meltwater erosion (Fig. 4a, b) and deglacial lithofacies (core Facies 3, AF2) with strong meltwater influence (Fig. 8c) appear to support such a scenario.

Despite the fact that the exact timing of margin retreat and the configuration of the margin in and around Disko Trough are not fully known, it is clear that topography was an important control on retreat in this system. The GZWs on the mid-shelf occur in an area where the trough narrows to around 20 km and the banks on the either side of the trough also shallow (Fig. 6). In addition, a more significant stillstand occurred near the head of the trough (this study, Rinterknecht et al., 2014) where shallow banks on either side of the trough and the basalt escarpment likely stabilised retreat (Fig. 9). However, at no point along the wide, straight Uummannaq Trough (cf. Fig. 1) was the flux of ice reduced naturally by a constriction in the trough profile that might have promoted a pause in retreat and GZW formation on the mid-shelf. Indeed, GZW formation there is thought to have been a result of a climatically-induced stillstand during the Bølling-Allerød transition and YD cold periods (Sheldon et al., 2016). In contrast, advance and retreat of the Disko outlet occurred during the YD (Ó Cofaigh et al., 2013a; Rinterknecht et al., 2014).

Thus, the implication of the new evidence of GrIS retreat presented here is that despite apparent regional similarities in the cross-shelf troughs offshore West Greenland (i.e. middle-shelf GZWs) and periods of rapid retreat via calving, it appears that the pattern of deglaciation in Disko Trough, once initiated, was heavily influenced by local controls on ice dynamics rather than regional climatic or oceanographic effects. In this trough, rapid deglaciation with several very brief pauses and then a more significant stillstand event shows that ice-stream retreat was heavily modulated by local topography around the dog-leg axis and bathymetric pinning points of the trough on the inner shelf. As ice in Disko Trough was stabilised by what must have been grounded ice on the banks we can also become more confident that grounded ice was indeed present on the shallow banks offshore central West Greenland during the LGM (see Fig. 9). This is in contrast to traditional LGM ice-sheet configurations in this area which cite terrestrial hinge-line and geomorphological evidence for ice-free areas on western Disko Ejland and the western part of the Nuussuaq Peninsula (Ingólfsson et al., 1990; Weidick and Bennike, 2007). If these areas were indeed ice free perhaps they existed as nunatuks, or were covered by thin, slow-flowing ice that may have extended to the shelf break (cf. Roberts et al., 2009). Alternatively, confluent fast-ice flow into Disko Trough on the shelf is thought to have been from Jakobsahavns Isbræ (through Disko Bugt) and areas south of the bay (Roberts and Long, 2005) (Fig. 9). Perhaps this ice flux was enough to feed the ice stream in Disko Trough without requiring that the western GrIS overtopped Disko Ejland; a similar drawdown of ice into the Uummannaq Trough from confluent ice streams draining the fjords was put forward by Roberts et al. (2013) to explain ice-free areas and coastal thinning of the ice sheet during deglaciation when marine areas still contained grounded ice. This could explain the discrepancies between marine and terrestrial dates around inner Disko Trough as well (cf. Fig. 9). Certainly, there is good offshore evidence for ice grounding on the Disko Banke up to a latitude of at least 69°30' N in the form of the large Hellefisk moraines (Brett and Zarudzki, 1979) and drainage onto the bank may have been through coastal depressions (see Fig. 1) thus bypassing (and not overtopping) Disko Ejland (Fig. 9).

There are still major uncertainties in the LGM ice-sheet configuration for much of central and north Greenland (cf. Funder et al., 2011), and additional discrepancies between the evidence and chronologies available from terrestrial and marine datasets of retreat and thinning histories. Here, we have used new evidence from the marine realm to further our knowledge of deglaciation in a major cross-shelf trough in West Greenland. Recent work shows that ice-stream retreat in Uummannaq Trough appears to have been responsive to climatic forcing and may have been influenced by oceanic warming (Sheldon et al., 2016), which is in stark contrast to deglaciation in Disko Trough. Therefore, the factors affecting ice retreat rates during the final deglaciation seem to have been individual to different West Greenland outlets with topographic controls on ice-sheet dynamics and ice-stream dynamics important locally and regional climatic drivers becoming dominant in the absence of significant topographic controls.

5. Conclusions

- Integrated marine geophysical (multibeam bathymetry and acoustic sub-bottom profiles) and geological (sediment cores) datasets from Disko Trough, West Greenland provide new evidence for how a major outlet of the GrIS retreated after the LGM. Lithofacies and radiocarbon dates indicate rapid retreat across the outer and middle shelf that progressed via calving. Retreat was interrupted on the middle shelf by several short-lived (tens of years) stillstands during which sediments built up at the grounded ice margin to form grounding-zone wedges (GZWs). The stillstands occurred at a narrowing of the trough, which reduced the ice flux from the outlet, temporarily stabilising the ice margin.
- A more major stillstand occurred on the inner shelf when ice was stabilised on a basalt escarpment running across the trough and possibly on the shallow banks (Disko and Store-Hellefiske banks) flanking the trough. Existing deglacial ages from the area show that the stillstand on the inner shelf occurred between ca. 12.2 and 11.1 ka but is unlikely to have lasted for this

whole period. The configuration of the ice margin on shallow banks and at the head of the trough likely promoted the formation of a calving bay over inner Disko Trough.

- During the stillstand periods of high subglacial meltwater influx alternated with times iceberg calving was dominant leading to the deposition of a characteristic mud-diamicton deglacial lithofacies, possibly related to summer-winter climate cycles. This is the first time that this lithofacies has been found on the continental shelf, which is probably a result of the confined ice-margin configuration (calving bay) and high basal melting established during deglaciation.

- Advance and retreat of a major West Greenland marine-terminating outlet in Disko Trough occurred during the Younger Dryas cold period. Stillstands during overall retreat occurred at topographic constrictions suggesting that once initiated the dominant controls on retreat in the trough were internal or local factors affecting ice dynamics. Large mid-shelf GZWs exist in cross-shelf troughs over a 900-km long stretch of the West Greenland shelf and are suggestive of a regional response of the GrIS during deglaciation, however, retreat of the Disko Trough outlet was modulated by topography and ice-dynamics rather than climatic or oceanic drivers. This study underlines importance of topographic effects during retreat of major outlets of GrIS in addition to regional drivers, and highlights the need for further deglacial history records from the Greenland continental shelf.

Acknowledgements

References

Alley, R.B., Blankenship, D.D., Bentley, C.R., Rooney, S.T., 1986. Deformation of till beneath ice stream B, West Antarctica. Nature 322, 57–59.

Anandakrishnan, S., Catania, G.A., Alley, R.B., Horgan, H.J., 2007. Discovery of till deposition at the grounding line of Whillans Ice Stream. Science 315, 1835–1838.

Anderson, J.B., 1999. Antarctic Marine Geology. Antarctic Marine Geology.

Andrews, J.T., Eberl, D., 2011. Surface (sea floor) and near-surface (box cores) sediment mineralogy in Baffin Bay as a key to sediment provenance and ice sheet variations. Can. J. Earth Sci. 48, 1307–1328.

Bamber, J.L., Vaughan, D.G., Joughin, I., 2000. Widespread complex flow in the interior of the Antarctic ice sheet. Science 287, 1248–1250.

Bennett, M.R., 2003. Ice streams as the arteries of an ice sheet: their mechanics, stability and significance. Earth-Science Rev. 61, 309–339.

Bennike, O., Björck, S., 2002. Chronology of the last recession of the Greenland ice sheet. J. Quat. Sci. 17, 211–219.

Björck, S., Bennike, O., Rosén, P., Andresen, C.S., Bohncke, S., Kaas, E., Conley, D., 2002. Anomalously mild Younger Dryas summer conditions in southern Greenland. Geology 30, 427–430.

Bonow, J.M., 2005. Re-exposed basement landforms in the Disko region, West Greenland—disregarded data for estimation of glacial erosion and uplift modelling. Geomorphology 72, 106–127.

Brett, C.P., Zarudzki, E.F.K., 1979. Project Westmar: a shallow marine geophysical survey on the West Greenland shelf. Rapp. Grønl. Geol. Unders. 87, 1–27.

Buch, E., 1981. The annual cycl of temperature, salinit, currents and water masses in Disko Bugt and adjacent waters, West Greenland, Medd. om Grøn. Biosci 5,

1–33.

Cai, J., Powell, R.D., Cowan, E.A., Carlson, P.R., 1997. Lithofacies and seismic-reflection interpretation of temperate glacimarine sedimentation in Tarr Inlet, Glacier Bay, Alaska. Mar. Geol. 143, 5–37.

Chalmers, J., Pulvertaft, T., Marcussen, C., Pedersen, A., 1999. New insight into the structure of the Nuussuaq Basin, central West Greenland. Mar. Petroleum Geol. 16, 197–224.

Christoffersen, P., Tulaczyk, S., Behar, A., 2010. Basal ice sequences in Antarctic ice stream: exposure of past hydrologic conditions and a principal mode of sediment transfer. J. Geophys. Res. Earth Surf. 115, 2003–2012.

Cowan, E.A., Cai, J., Powell, R.D., Clark, J.D., Pitcher, J.N., 1997. Temperate glacimarine varves: an example from Disenchantment Bay, Southern Alaska. J. Sed. Res. 67, 536–549.

Dahl-Jensen, D., Mosegaard, K., Gundestrup, N., Clow, G.D., Johnsen, S.J., Hansen, A.W., Balling, N., 1998. Past temperatures directly from the Greenland ice sheet. Science 282, 268–271.

Domack, E., Duran, D., Leventer, A., Ishman, S., Doane, S., McCallum, S., Amblas, D., Ring, J., Gilbert, R., Prentice, M., 2005. Stability of the Larsen B ice shelf on the Antarctic Peninsula during the Holocene epoch. Nature 436, 681–685.

Domack, E.W., Jacobson, E.A., Shipp, S., Anderson, J.B., 1999. Late Pleistocene–Holocene retreat of the West Antarctic ice-sheet system in the Ross Sea: part 2—sedimentologic and stratigraphic signature. Geol. Soc. Am. Bull. 111, 1517–1536.

Domack, E.W., McClennen, C.E., 1996. Accumulation of glacial marine sediments in fjords of the Antarctic Peninsula and their use as Late Holocene Paleoenvironmental indicators. Foundations for Ecological research west of the Antarctic Peninsula, Ant. Res. Ser. 70, 135–154.

Dowdeswell, J., Fugelli, E., 2012. The seismic architecture and geometry of grounding-zone wedges formed at the marine margins of past ice sheets. Geol. Soc. Am. Bull. 124, 1750–1761.

Dowdeswell, J., Ottesen, D., Evans, J., Ó Cofaigh, C., Anderson, J., 2008. Submarine glacial landforms and rates of ice-stream collapse. Geology 36, 819–822.

Dowdeswell, J., Whittington, R., Jennings, A., Andrews, J., Mackensen, A., Marienfeld, P., 2000. An origin for laminated glacimarine sediments through sea-ice build-up and suppressed iceberg rafting. Sedimentology 47, 557–576.

Dowdeswell, J.A., Evans, J., Ó Cofaigh, C., 2010. Submarine landforms and shallow acoustic stratigraphy of a 400 km-long fjord-shelf-slope transect, Kangerlussuaq margin, East Greenland. Quat. Sci. Rev. 29, 3359–3369.

Dowdeswell, J.A., Hogan, K.A., Ó Cofaigh, C., Fugelli, E.M.G., Evans, J., Noormets, R., 2014. Late quaternary ice flow in a West Greenland fjord and cross-shelf trough system: submarine landforms from Rink Isbrae to Uummannaq shelf and slope. Quat. Sci. Rev. 92, 292–309.

Evans, J., Dowdeswell, J.A., Grobe, H., Niessen, F., Stein, R., Hubberten, H.-W., Whittington, R., 2002. Late Quaternary Sedimentation in Kejser Franz Joseph Fjord and the Continental Margin of East Greenland, 203. Geological Society, London, pp. 149–179. Special Publications.

Evans, J., Ó Cofaigh, C., Dowdeswell, J.A., Wadhams, P., 2009. Marine geophysical evidence for former expansion and flow of the Greenland ice sheet across the north-east Greenland continental shelf. J. Quat. Sci 24, 279–293.

Evans, J., Pudsey, C.J., Ó Cofaigh, C., Morris, P., Domack, E., 2005. Late Quaternary glacial history, flow dynamics and sedimentation along the eastern margin of the Antarctic Peninsula Ice Sheet. Quat. Sci. Rev. 24, 741–774.

Eyles, N., Eyles, C.H., Miall, A.D., 1983. Lithofacies types and vertical profile models; an alternative approach to the description and environmental interpretation of glacial diamict and diamictite sequences. Sedimentology 30, 393–410.

Funder, S., 1989. Quaternary geology of the ice-free areas and adjacent shelves of Greenland. In: Fulton, R.J. (Ed.), Quaternary Geology of Canada and Greenland. Geological Survey of Canada, pp. 743–792.

Funder, S., Hansen, L., 1996. The Greenland ice sheet — a model for its culmination and decay during and after the last glacial maximum. Bull. Geol. Soc. Den. 42, 137–152.

Funder, S., Kjeldsen, K.K., Kjær, K.H., Ó Cofaigh, C., 2011. The Greenland ice sheet during the Past 300,000 years: a review. In: Ehlers, J., Gibbard, P., Hughes, P. (Eds.), Quaternary Glaciations – Extent and Chronology. Part IV: a Closer Look, pp. 699–713.

Funder, S., Larsen, H.C., 1989. Quaternary geology of the shelves adjacent to Greenland. In: Fulton, R.J. (Ed.), Quaternary Geology of Canada and Greenland. Geological Survey of Canada.

Gilbert, R., 2000. Environmental assessment from the sedimentary record of high-latitude fiords. Geomorphology 32, 295–314.

Graham, A.G.C., Hogan, K.A., Crescentic scours on palaeo-ice stream beds, in: Dowdeswell, J.A., Canals, M., Todd, B.J., Jakobsson, M., Dowdeswell, E.K., Hogan, K.A. (Eds.), The Atlas of Submarine Glacial Landforms, Geological Society of London Memoir 46, (in press).

Grobe, H., 1987. A simple method for the determination of ice-rafted debris in sediment cores. Polarforschung 57, 123–126.

Henderson, G., 1975. New bathymetric maps Covering Offshore West Greenland 59*-69*30′N. Offshore Technology Conference.

Hofman, J.C., Knutz, P.C., 2015. Seismic stratigraphic architecture of the Disko Bay trough-mouth fan system, West Greenland. Geophys. Res. Abstr 17. EGU2015–11588, EGU General Assembly 2015.

Hofman, J.C., Knutz, P.C., Nielsen, T., Kjuipers, A., 2016. Seismic architecture and evolution of the Disko Bay trough-mouth fan, central West Greenland margin 147, 69–90.

Hogan, K.A., Dowdeswell, J.A., Noormets, R., Evans, J., Ó Cofaigh, C., Jakobsson, M.,

2010. Submarine landforms and ice-sheet flow in the Kvitøya Trough, north-western Barents Sea. Quat. Sci. Rev. 29, 3545—3562.

Hogan, K.A., Dowdeswell, J., Ó Cofaigh, C., 2012. Glacimarine sedimentary processes and depositional environments in an embayment fed by West Greenland ice streams. Mar. Geol. 311, 1—16.

Hogan, K.A., Dix, J.K., Lloyd, J.M., Long, A.J., Cotterill, C.J., 2011. Seismic stratigraphy records the deglacial history of Jakobshavn Isbræ, West Greenland. J. Quat. Sci. 26, 757.

Ingólfsson, Ó., Frich, P., Funder, S., Humlum, O., 1990. Paleoclimatic implications of an early Holocene glacier advance on Disko Island, West Greenland. Boreas 19, 297—311.

Jakobsson, M., Anderson, J.B., Nitsche, F.O., Gyllencreutz, R., Kirshner, A.E., Kirchner, N., O'Regan, M., Mohammad, R., Eriksson, B., 2012. Ice sheet retreat dynamics inferred from glacial morphology of the central Pine Island Bay Trough, West Antarctica. Quat. Sci. Rev. 38, 1—10.

Jamieson, S.S., Vieli, A., Ó Cofaigh, C., Stokes, C.R., Livingstone, S.J., Hillenbrand, C.D., 2014. Understanding controls on rapid ice-stream retreat during the last deglaciation of Marguerite Bay, Antarctica, using a numerical model. J. Geophys. Res. Earth Surf. 119, 247—263.

Jennings, A.E., Helgadóttir, G., 1994. Foraminiferal assemblages from the fjords and shelf of eastern Greenland. J. Foraminifer. Res. 24, 123—144.

Jennings, A.E., Walton, M.E., Ó Cofaigh, C., Kilfeather, A., Andrews, J.T., Ortiz, J.D., De Vernal, A., Dowdeswell, J.A., 2013. Paleoenvironments during younger Dryas-early Holocene retreat of the Greenland ice sheet from outer Disko trough, central west Greenland. J. Quat. Sci. 29, 27—40.

Jennings, A.E., Weiner, N.J., 1996. Environmental change in eastern Greenland during the last 1300 years: evidence from foraminifera and lithofacies in Nansen Fjord, 68 N. Holocene 6, 179—191.

Joughin, I., Abdalati, W., Fahnestock, M., 2004. Large fluctuations in the speed on Greenland's Jakobshavn Isbrae glacier. Nature 432, 608—610.

Joughin, I., Rignot, E., Rosanova, C.E., Lucchitta, B.K., Bohlander, J., 2003. Timing of recent accelerations of Pine island Glacier, Antarctica. Geophys. Res. Lett. 30, 4.

Kelley, S.E., Briner, J.P., Young, N.E., 2013. Rapid ice retreat in Disko Bugt supported by 10 Be dating of the last recession of the western Greenland Ice Sheet. Quat. Sci. Rev. 82, 13—22.

Kelley, S.E., Briner, J.P., Zimmerman, S.R.H., 2015. The influence of ice marginal setting on early Holocene retreat rates in central West Greenland. J. Quat. Sci. 30, 271—280.

Kelly, M., 1985. A review of the Quaternary geology of western Greenland. In: Andrews, J.T. (Ed.), Quaternary Environments Eastern Canadian Arctic, Baffin Bay, Western Greenland. Allen & Unwin, Boston, pp. 461—501.

Khan, S.A., Wahr, J., Bevis, M., Velicogna, I., Kendrick, E., 2010. Spread of ice mass loss into northwest Greenland observed by GRACE and GPS. Geophys. Res. Lett. 37.

Kilfeather, A.A., Ó Cofaigh, C., Lloyd, J.M., Dowdeswell, J.A., Xu, S., Moreton, S.G., 2011. Ice-stream retreat and ice-shelf history in Marguerite Trough, Antarctic Peninsula: Sedimentological and foraminiferal signatures. Geol. Soc. Am. Bull. 123, 997—1015.

Kleiber, H.P., Knies, J., Niessen, F., 2000. The Late Weichselian glaciation of the Franz Victoria Trough, northern Barents Sea: ice sheet extent and timing,. Mar. Geol. 168, 25—44.

Larsen, J.G., Pulvertaft, T.C.R., 2000. The structure of the Cretaceous-Palaeogene sedimentary-volcanic area of Svartenhuk Halvø, central West Greenland. Geol. Surv. Den. Greenl. Ministry Environ. Energy 188, 40.

Larter, R., Vanneste, L., 1995. Relict subglacial deltas on the Antarctic Peninsula outer shelf. Geology 23, 33—36.

Lloyd, J.M., Moros, M., Perner, K., Telford, R.J., Kuijpers, A., Jansen, E., McCarthy, D., 2011. A 100 yr recrod of ocean temperature control on the stability of Jakobshavn Isbrae, West Greenland. Geology 39, 867—870.

Lloyd, J.M., Park, L.A., Kuijpers, A., Moros, M., 2005. Early Holocene palaeo-oceanography and deglacial chronology of Disko bugt, west Greenland. Quat. Sci. Rev. 24, 1741—1755.

Long, A.J., Roberts, D.H., 2002. A revised chronology for the 'Fjord Stade' moraine in Disko Bugt, west Greenland. J. Quat. Sci. 17, 561—579.

Long, A.J., Roberts, D.H., 2003. Late Weichselian deglacial history of Disko Bugt, West Greenland, and the dynamics of the Jakobshavns Isbrae ice stream. Boreas 32, 208—226.

McCarthy, D.J., 2011. Late Quaternary Ice-ocean Interactions in Central West Greenland. Department of Geography. Durham University, p. 292.

Moon, T., Joughin, I., 2008. Changes in ice front position on Greenland's outlet glaciers from 1992 to 2007. J. Geophys. Res. Earth Surf. 113, 2003—2012.

Nick, F.M., Vieli, A., Andersen, M.L., Joughin, I., Payne, A., Edwards, T.L., Pattyn, F., van de Wal, R.S., 2013. Future sea-level rise from Greenland/'s main outlet glaciers in a warming climate. Nature 497, 235—238.

Ó Cofaigh, C., Andrews, J., Jennings, A., Dowdeswell, J., Hogan, K., Kilfeather, A., Sheldon, C., 2013b. Glacimarine lithofacies, provenance and depositional processes on a West Greenland trough-mouth fan. J. Quat. Sci. 28, 13—26.

Ó Cofaigh, C., Dowdeswell, J.A., Allen, C.S., Hiemstra, J.F., Pudsey, C.J., Evans, J., Evans, D.J., 2005. Flow dynamics and till genesis associated with a marine-based Antarctic palaeo-ice stream. Quat. Sci. Rev. 24, 709—740.

Ó Cofaigh, C., Dowdeswell, J.A., Jennings, A.E., Hogan, K.A., Kilfeather, A.A., Hiemstra, J.F., Noormets, R., Evans, J., McCarthy, D.J., Andrews, J.T., Lloyd, J.M., Moros, M., 2013a. An extensive and dynamic ice sheet on the West Greenland shelf during the last glacial cycle. Geology 41, 219—222.

Ó Cofaigh, C., Pudsey, C.J., Dowdeswell, J.A., Morris, P., 2002. Evolution of subglacial

bedforms along a paleo-ice stream, Antarctic Peninsula continental shelf. Geophys. Res. Lett. 29, 41—44.

Ottesen, D., Dowdeswell, J., 2006. Assemblages of submarine landforms produced by tidewater glaciers in Svalbard. J. Geophys. Res. Earth Surf. (2003—2012) 111.

Ottesen, D., Dowdeswell, J., Rise, L., 2005. Submarine landforms and the reconstruction of fast-flowing ice streams within a large quaternary ice sheet: the 2500-km-long Norwegian-Svalbard margin (57—80 N). Geol. Soc. Am. Bull. 117, 1033—1050.

Ottesen, D., Dowdeswell, J.A., Landvik, J.Y., Mienert, J., 2007. Dynamics of the Late Weichselian ice sheet on Svalbard inferred from high-resolution sea-floor morphology. Boreas-Int. J. Quat. Res. 36, 286—306.

Perner, K., Moros, M., Jennings, A., Lloyd, J.M., Knudsen, K.L., 2012. Holocene Palaeoceanographic Evolution off West Greenland. The Holocene, 0959683612460785.

Perner, K., Moros, M., Lloyd, J., Kuijpers, A., Telford, R., Harff, J., 2011. Centennial scale benthic foraminiferal record of late Holocene oceanographic variability in Disko Bugt, West Greenland. Quat. Sci. Rev. 30, 2815—2826.

Polyak, L., Solheim, A., 1994. Late-and postglacial environments in the northern Barents Sea west of Franz Josef Land. Polar Res. 13, 197—207.

Quillmann, U., Jennings, A.E., Bendle, J., Jonsdóttir, H., Kristjansdóttir, G.B., Lloyd, J., Ólafsdóttir, S., Principato, S., 2009. Radiocarbon Date List XI: Radiocarbon Dates from Marine Sediment Cores of the Iceland, Greenland, and Northeast Canadian Arctic Shelves and Nares Strait, 59. Occasional Paper - Colorado University, Institute of Arctic and Alpine Research, p. 69.

Rasmussen, S.O., Andersen, K.K., Svensson, A., Steffensen, J.P., Vinther, B.M., Clausen, H.B., Siggaard-Andersen, M.L., Johnsen, S.J., Larsen, L.B., Dahl-Jensen, D., 2006. A new Greenland ice core chronology for the last glacial termination. J. Geophys. Res. Atmos. 111, 1984—2012.

Reimer, P.J., Bard, E., Bayliss, A., Beck, J.W., Blackwell, P.G., Bronk Ramsey, C., Buck, C.E., Cheng, H., Edwards, R.L., Friedrich, M., 2013. IntCal13 and Marine13 Radiocarbon Age Calibration Curves 0—50,000 Years cal BP.

Ribergaard, M.H., Buch, E., 2008. Oceanographic investigations off west Greenland 2007. NAFO Sci. Council Doc 7 (003).

Rignot, E., Kanagaratnam, P., 2006. Changes in the velocity structure of the Greenland ice sheet. Science 311, 986—990.

Rignot, E., Mouginot, J., Morlighem, M., Seroussi, H., Scheuchl, B., 2014. Widespread, rapid grounding line retreat of Pine Island, Thwaites, Smith, and Kohler glaciers, West Antarctica, from 1992 to 2011. Geophys. Res. Lett. 41, 3502—3509.

Rinterknecht, V., Jomelli, V., Brunstein, D., Favier, V., Masson-Delmotte, V., Bourlès, D., Leanni, L., Schläppy, R., 2014. Unstable ice stream in Greenland during the Younger Dryas cold event. Geology 42, 759—762.

Roberts, D.H., Long, A.J., 2005. Streamlined bedrock terrain and fast ice flow, Jakobshavns Isbrae, West Greenland: implications for ice stream and ice sheet dynamics. Boreas 34, 25—42.

Roberts, D.H., Long, A.J., Davies, B.J., Simpson, M.J., Schnabel, C., 2010. Ice stream influence on West Greenland ice sheet dynamics during the last glacial maximum. J. Quat. Sci. 25, 850—864.

Roberts, D.H., Rea, B.R., Lane, T.P., Schnabel, C., Rodés, A., 2013. New constraints on Greenland ice sheet dynamics during the last glacial cycle: evidence from the Uummannaq ice stream system. J. Geophys. Res. Earth Surf. 118, 519—541.

Roberts, D.H., Long, A.J., Lloyd, J.M., Schnabel, C., Davies, B.J., Xu, S., Simpson, M.J.R., Huybrechts, P., 2009. Ice sheet extent and early deglacial history of the southwestern sector of the Greenland Ice Sheet. Quat. Sci. Rev. 28, 2760—2773.

Roksandic, M.M., 1979. Geology of the continental shelf off West Greenland between 61°15′N and 64°00′N. Grønl. Geol. Unders. 92, 15.

Rolle, F., 1985. Late Cretaceous-Tertiary sediments offshore central West Greenland: lithostratigraphy, sedimentary evolution, and petroleum potential. Can. J. Earth Sci. 22, 1001—1019.

Ryan, J.C., Dowdeswell, J.A., Hogan, K.A., Three cross-shelf troughs on the continental shelf of Southwest Greenland from Olex data, in: Dowdeswell, J.A., Canals, M., Todd, B.J., Jakobsson, M., Dowdeswell, E.K., Hogan, K.A. (Eds.), The Atlas of Submarine Glacial Landforms, Geological Society of London Memoir 46, (in press).

Rydningen, T.A., Vorren, T.O., Laberg, J.S., Kolstad, V., 2013. The marine-based Fennoscandian ice sheet: glacial and deglacial dynamics as reconstructed from submarine landforms. Quat. Sci. Rev. 68, 126—141.

Schoof, C., 2007. Ice sheet grounding line dynamics: steady states, stability, and hysteresis. J. Geophys. Res. Earth Surf. 112, 2003—2012.

Sheldon, C., Jennings, A.E., Andrews, J.T., Ó Cofaigh, C., Hogan, K.A., Seidenkrantz, M.-S., Dowdeswell, J.A., 2016. Ice Stream retreat following the LGM and development onset of the West Greenland Current in the Uummannaq Trough System, West Greenland. Quat. Sci. Rev. 147, 27—46.

Schafer, C.T., Cole, F.E., 1986. Reconnaissance survey of benthonic foraminifera from Baffin Island fiord environments. Arctic 39, 232—239.

Shreve, R., 1972. Movement of water in glaciers. J. Glaciol. 11, 205—214.

Smith, L.M., Andrews, J.T., 2000. Sediment characteristics in iceberg dominated fjords, Kangerlussuaq region, East Greenland. Sediment. Geol. 130, 11—25.

Stuiver, M., Reimer, P.J., Reimer, R.W., 2015. CALIB 7.1. Available online at: calib.qub.ac.uk/calib.

Tulaczyk, S.M., Scherer, R.P., Clark, C.D., 2001. A ploughing model for the origin of weak tills beneath ice streams: a qualitative treatment. Quat. Int. 86, 59—70.

Ullrich, A.D., Cowan, E.A., Zellers, S.D., Jaeger, J.M., Powell, R.D., 2009. Intra-annual variability in benthic foraminiferal abundance in sediments of Disenchantment Bay, an Alaskan glacial fjord. Arct. Antarct. Alp. Res. 41, 257—271.

van Tatenhove, F.G., van der Meer, J.J., Koster, E.A., 1996. Implications for

deglaciation chronology from new AMS age determinations in central West Greenland. Quat. Res. 45, 245–253.

Velicogna, I., 2009. Increasing rates of ice mass loss from the Greenland and Antarctic ice sheets revealed by GRACE. Geophys. Res. Lett. 36.

Vorren, T.O., Hald, M., Thomsen, E., 1984. Quaternary sediments and environments on the continental shelf off northern Norway. Mar. Geol. 57, 229–257.

Weertman, J., 1974. Stability of the junction of an ice sheet and an ice shelf. J. Glaciol. 13, 3–11.

Weidick, A., 1972. Holocene shore-lines and glacial stages in Greenland – an attempt at correlation. Rapp. Grønl. Geol. Unders. 41, 39.

Weidick, A., Bennike, O., 2007. Quaternary glaciation history and glaciology of Jakobshavn Isbræ and the Disko Bugt region, West Greenland: a review. Geol. Surv. Den. Greenl. 14, 78.

Weidick, A., Kelly, M., Bennike, O., 2004. Late Quaternary development of the southern sector of the Greenland Ice Sheet, with particular reference to the Qassimiut lobe. Boreas-Int. J. Quat. Res. 33, 284–299.

Whittaker, R.C., 1996. A preliminary seismic investigation of an area with extrusive Tertiary basalts offshore central West Greenland,. Bull. Grøn. Geol. Under 172, 28–31.

Winkelmann, D., Jokat, W., Jensen, L., Schenke, H.W., 2010. Submarine end moraines on the continental shelf off NE Greenland – implications for Lateglacial dynamics. Quat. Sci. Rev. 29, 1069–1077.

Young, N.E., Briner, J.P., Axford, Y., Csatho, B., Babonis, G.S., Rood, D.H., Finkely, R.C., 2011. Response of a marine terminating Greenland outlet glacier to abrupt cooling 8200 and 9300 years ago. Geophys. Res. Lett. 38, L24701.

Young, N.E., Briner, J.P., Rood, D.H., Finkel, R.C., Corbett, L.B., Bierman, R., 2013. Age of the Fjord Stade moraines in the Disko Bugt region, western Greenland, and the 9.3 and 8.2 ka cooling events. Quat. Sci. Rev. 60, 76–90.